THE ASTROPHYSICAL JOURNAL, 445:789–810, 1995 June 1

AN EXTENDED GRID OF MULTICYCLE NOVA EVOLUTION MODELS

DINA PRIALNIK[1,2] AND ATTAY KOVETZ[1,2,3]
Received 1994 August 15; accepted 1994 December 6

ABSTRACT

According to the nova theory, observed characteristics of novae may be reproduced by varying the values of three basic and independent parameters: the accreting white dwarf's mass M_{WD}, its temperature T_{WD}, and the mass transfer rate $\dot{M}$. Calculations performed to date have, however, left wide regions of the parameter space unexplored.

We carry out a systematic study involving calculations of evolutionary sequences of nova outbursts through several cycles, for 64 parameter combinations spanning the entire parameter space, assuming CO white dwarfs (WDs). An updated stellar evolution code is used, including an extended nuclear reactions network, new opacities (OPAL), diffusion of all elements and the effect of radiation pressure on mass loss. We find that the entire range of observed nova characteristics can be accounted for, including recurrent and symbiotic novae. Recurrent novae may be obtained on relatively low-mass WDs ($\sim 1\ M_\odot$). Accretion at rates $\dot{M} \geq 10^{-7}\ M_\odot\ \mathrm{yr}^{-1}$ invariably results in an increase of M_{WD} and may, eventually, lead to a type Ia supernova. For accretion rates $\dot{M} \leq 10^{-9}\ M_\odot\ \mathrm{yr}^{-1}$, M_{WD} decreases under all circumstances. The overall dependence of nova characteristics on the basic parameters is analyzed. Observed correlations between nova properties, as well as the conspicuous lack of correlation between other properties, are verified by the theoretical results.

Among all the observed properties of novae there are three that appear to be independent of each other: the time of decline by 3 magnitudes t_3, the heavy element abundance of the ejecta Z_{ej}, and their helium content Y_{ej}. Our calculations yield $t_3(M_{WD}, T_{WD}, \dot{M})$, $Z_{ej}(M_{WD}, T_{WD}, \dot{M})$, $Y_{ej}(M_{WD}, T_{WD}, \dot{M})$ at discrete points over the entire parameter space. By matching observed characteristics of a particular nova with calculated counterparts, it is possible to derive the WD's mass and temperature and the (average) accretion rate as well as additional observable properties. We find an excellent match for the measured expansion velocities, but the calculated ejected masses are generally smaller than those estimated from observations.

Subject headings: accretion, accretion disks — binaries: close — novae, cataclysmic variables — stars: interiors — white dwarfs

1. INTRODUCTION

The nova theory may perhaps be considered the greatest advance in stellar evolution during the past two decades. It has emerged from numerous theoretical studies (e.g., Starrfield, Sparks, & Truran 1974a, b; Prialnik, Shara, & Shaviv 1978, 1979; see also reviews by Shara 1989 and by Livio 1994), which showed that the typical features of novae could result from transfer of hydrogen-rich material onto a white dwarf (WD), leading to a thermonuclear runaway (TNR). The large variation in the observed features—the peak luminosity, the amount, composition and average expansion velocity of the ejected matter, or the duration of the high-luminosity phase—is attributed by the nova theory to differences in the values assumed for three basic parameters: the accreting WD's mass M_{WD}, its temperature T_{WD} (or, equivalently, its luminosity or age), and the mass transfer rate $\dot{M}$ (MacDonald 1983; Kovetz & Prialnik 1985; Prialnik 1993, and references therein).

Thus, each observed nova exhibits a particular combination of many different properties, and nova theory postulates that there exists a set of values for the three basic parameters M_{WD}, T_{WD}, and $\dot{M}$ that should reproduce these properties in a numerical evolutionary calculation. We do not know, however, how to choose the primitive parameters that would result in a particular combination observed. More importantly, we do not know whether *all* observed combinations *can* be obtained, i.e., whether the nova theory, in its present state, is complete. For example, a high Z, combined with a very slow decline (e.g., Nova DQ Her) seem to be contradictory from the point of view of the theory. But perhaps this is simply because certain parts of the parameter space (low M_{WD}, high T_{WD}) have not been explored. Moreover, it is not clear whether the entire extent of parameter space required in order to accommodate the observations of classical novae is compatible with stellar evolution theory in general. The mass transfer rate, for example, even if acceptable from the point of view of nova theory, must still be compatible with the properties of the binary system and with the nature of the secondary star (which must be of smaller mass than the primary, and in an earlier stage of evolution).

In spite of the success of the nova theory in reproducing the wide range of variation for most of the observed features of novae, there are still open questions:

1. Can the peculiar compositions deduced from nova spectra, in particular the *simultaneous* enrichment of helium and heavier elements (Truran 1990), be accounted for by suitable, and realistic, combinations of the basic parameters?

2. What are the ranges of M_{WD} and $\dot{M}$ that lead to classical nova (CN) eruptions, and how do they compare to the sparse observational data regarding M_{WD} and the values of $\dot{M}$ derived from accretion disk models (e.g., Patterson 1984; Warner 1987) and from observations of old novae (Shara et al. 1984; Shara, Moffat, & Webbink 1985)?

3. Is it possible to extend the parameter range leading to

[1] Space Telescope Science Institute, 3700 San Martin Drive, Baltimore, MD 21218.
[2] Department of Geophysics and Planetary Sciences.
[3] School of Physics and Astronomy, Raymond and Beverly Sackler Faculty of Exact Sciences, Tel Aviv University, Ramat Aviv 69978, Israel.

recurrent novae (RNs) to WD masses that are substantially less than the Chandrasekhar limiting mass? Only a few theoretical studies (Starrfield, Sparks, & Truran 1985; Starrfield, Sparks, & Shaviv 1988; Truran et al. 1988; Kato 1990, 1991; Kovetz & Prialnik 1994) have produced model candidates for RNs. All of them assumed an M_{WD} of about 1.4 $M_\odot$—which is uncomfortably close to the Chandrasekhar limit—and a high accretion rate (which is essential for frequent eruptions). Not all of the observed characteristics of RNs could be reproduced in this way. It would therefore be desirable to extend the search for model candidates to a wider range of parameter space. Whether a RN can be produced by a WD of about 1.0 $M_\odot$ is still unknown.

4. What are the conditions required for an accreting WD to retain some of the accreted material and hence grow in mass? Could it reach the Chandrasekhar mass limit before the companion is exhausted, so as to qualify as a Type Ia supernova progenitor (e.g., Whelan & Iben 1973; Wheeler 1992; Livio 1995)? It is a priori clear that these requirements must impose severe restrictions on the values of the three basic parameters.

All these questions could be answered by a comprehensive study of accretion onto white dwarfs, provided that it is carried out in a systematic way, and so as to cover the entire range of parameters. The ultimate test of nova theory can only be provided by such a study, which would be similar to the systematic evolutionary calculations that aim at reproducing the HR-diagrams of globular clusters. This is the main objective of this work.

A project of this kind must overcome three major difficulties. First, a great number of evolutionary calculations is needed in order to span the required ranges of the three basic parameters. Only a few sets of calculations involving changes in *all three* parameters have ever been attempted (e.g., Kovetz & Prialnik 1985; Iben, Fujimoto, & MacDonald 1992; Schwartzman, Kovetz, & Prialnik 1994), but they were not multicycle, or even full-cycle, calculations; and their coverage of parameter space was rather sparse. Such calculations cannot determine the mass retained after the mass-loss phase, nor the degree of helium enrichment, for which at least two evolutionary cycles are necessary. But even these limited studies revealed some new and unforeseen effects.

Secondly, a computer code is required which can follow evolutionary phases—accretion, thermonuclear runaway, expansion, mass loss—that differ radically in time scales and physical processes considered: element diffusion, extensive network of nuclear reactions, dynamic expansion, wind. The first calculation of a full nova cycle was done by Prialnik (1986). Partly as a result of that study a new procedure for calculating mass-loss was developed by Prialnik & Kovetz (1992).

Thirdly, a *real* nova cycle starts from initial conditions—density, temperature, and abundance profiles—that are the final outcome of a previous cycle. These cannot be correctly guessed at the outset of a calculation. It is therefore necessary to follow a number of full nova cycles, until a repetitive pattern is obtained. Two such multicycle sequences were calculated (Shara, Prialnik, & Kovetz 1993; Kovetz & Prialnik 1994), and they conclusively demonstrated that arbitrary chosen initial conditions were in fact unrepresentative, and that a regular cycle pattern was only established after several cycles. The composition of the ejecta was found to be particularly affected, while other characteristics differed by no more than 10%–20% between the first cycle and a regular one.

We have thus undertaken the calculation of a series of full, multicycle evolutionary sequences, spanning a sufficiently dense grid of the three basic parameters M_{WD}, T_{WD}, and $\dot{M}$, using an updated hydrodynamical stellar evolution code (A. Kovetz, unpublished). In this paper we report the general results of these calculations, without going into the details of the evolution. Apart from constituting a comprehensive test of the nova theory, a somewhat more ambitious aim of this project is to provide a method for answering the inverse problem: given a set of observed characteristics for a particular nova, what are its parameters M_{WD}, $\dot{M}$, and T_{WD} (which would be extremely difficult, or impossible, to obtain by direct observation)? In § 2 we describe the improvements introduced in the code and the method of calculation; we also justify the choice of parameters, based on observations and previous calculations. In § 3 we present the results and analyze them by determining the maximum span of different properties, the effect of each parameter, i.e., the trend of change of nova characteristics with each of the basic parameters. In § 4 we discuss our results in the light of observations; we seek correlations (or lack thereof) similar to the observed ones and we identify different classes of novae by matching the defining properties of these classes to our models. Finally, in § 5 we summarize the main conclusions and we also attempt to answer the questions posed above. We defer a detailed comparison between our models and different nova classes (recurrent, symbiotic, and classical) to a series of future papers.

2. METHOD OF COMPUTATION

2.1. *Update of the Computation Code*

The hydrodynamic stellar evolution code used has been updated to include new opacities, an extended nuclear reactions network and a modified mass-loss algorithm.

1. The important role which the radiative opacity plays in the final stages of nova mass loss has been recently stressed by Kato & Iben (1992). The latest OPAL opacity tables calculated by F. J. Rogers & C. A. Iglesias (1993, private communication) have been incorporated in the code.

2. Under extreme conditions, novae can reach temperatures of several hundred million degrees at the peak of the TNR. At such temperatures breakout from the CNO cycle of hydrogen burning is expected to occur, with rapid build-up of heavy elements by proton captures on the one hand, and the subsequent inverse-beta decays of such elements on the other. The nuclear reactions network has therefore been extended and it now includes 40 heavy elements: ^{12}C, ^{13}C, ^{14}C, ^{13}N, ^{14}N, ^{15}N, ^{14}O, ^{15}O, ^{16}O, ^{17}O, ^{18}O, ^{17}F, ^{18}F, ^{19}F, ^{18}Ne, ^{19}Ne, ^{20}Ne, ^{21}Ne, ^{22}Ne, ^{20}Na, ^{21}Na, ^{22}Na, ^{23}Na, ^{22}Mg, ^{23}Mg, ^{24}Mg, ^{25}Mg, ^{26}Mg, ^{24}Al, ^{25}Al, ^{26}Al, ^{27}Al, ^{27}Si, ^{28}Si, ^{29}Si, ^{30}Si, ^{28}P, ^{29}P, ^{30}P, ^{31}P and the p, α, n, and γ exchanges between them (Caughlan & Folwler 1988).

3. Our hydrodynamical code is Lagrangian, therefore mass-conserving. Left to itself, it will follow the evolution of a mass-losing star to infinite radii. Eventually it will encounter numerical difficulties, but this will usually happen long after one of the assumptions on which it is based—for example, radiative diffusion—is violated. In principle, one should contemplate a method by which the Lagrangian hydrodynamical code is matched, at some suitable point below the surface, to another one that describes a wind solution. But we have noticed that, following the phase of rapid expansion, our code as a matter of fact produces an expanding outer zone which is

supersonic, and in which $4\pi r^2 \rho v$ is spatially uniform; in other words, a steady, optically thick, supersonic wind solution. In order to identify such cases, and to determine the appropriate mass-loss rate, we have used the following mass loss algorithm (see Prialnik & Kovetz 1992; Kovetz & Prialnik 1994): noting the well known steady wind equations (in standard notation)

$$\dot{m} = 4\pi r^2 \rho v = \text{constant}\,, \tag{1}$$

$$(v^2 - c_s^2)\frac{1}{v}\frac{dv}{dr} = \frac{2c_s^2}{r} - \left(1 - \frac{\partial P/\partial \log T}{4P_{\rm rad}}\frac{L_{\rm rad}}{L_{\rm Edd}}\right)\frac{Gm}{r^2}\,, \tag{2}$$

where the squared (isothermal) sound speed and the Eddington luminosity are defined by

$$c_s^2 = \frac{\partial P_{\rm gas}}{\partial \rho}\,, \quad L_{\rm Edd} = \frac{4\pi cGm}{\kappa}\,, \tag{3}$$

the algorithm tests for an outer (subsurface) zone being in the supersonic wind regime, where $v > c_s$ and the right-hand side of equation (2) is positive. If such a zone exists, the mass-loss rate is calculated from equation (1), evaluated at the bottom of the zone. An amount $\dot{m}\delta t$, where δt is the time step, is subtracted from the outermost mass shell Δm_S. The time step is constrained during this phase by the requirement that $\dot{m}\delta t$ be a fraction of Δm_S. Whenever Δm_S becomes very small, it is merged with the underlying mass shell. For reassurance, the code also tests the constancy of $4\pi r^2 \rho v$ throughout the zone; whenever the number of shells in the wind zone was greater than, 2, this quantity was constant to within a few percent. Our previous mass loss algorithms did not include the "radiation pressure" correction factor multiplying Gm/r^2 in equation (2).

4. Diffusion was computed for all elements. Those that had mass fractions less than 0.003 were treated as traces and their diffusion velocities were calculated by taking account of their collisions with the more abundant species (i.e., neglecting collisions among traces; Kovetz & Shaviv 1994).

Accretional heating was taken into account, assuming an accretion luminosity (Regev & Shara 1989)

$$L_{\rm acc} = 0.15GM_{\rm WD}\dot{M}/R_{\rm WD}\,. \tag{4}$$

Convective fluxes were calculated according to the mixing length theory, with the constants of Mihalas (1978), adopting a mixing length to pressure scale height ratio of 2. Since the mixing length theory is based on hydrostatic equilibrium, convection was turned off whenever kinetic energies or accelerations became significant. This happened only in the outer layers of the model, during the dynamic mass loss phase, when convective heat transport was inefficient. Prior to this phase, convection had already reached the surface of the star and produced a uniform envelope composition. Thus, convection was suppressed under circumstances in which it had no significant effect on the evolution.

2.2. *Determination of the Parameter Space*

In this study we have only considered CO WDs; all models had an identical homogeneous composition of C and O in equal mass fractions. The WD mass range adopted was 0.65 to 1.40 $M_\odot$. Analytic relations that provide the trend of change of nova characteristics with the WD mass (e.g., Fujimoto 1982a; Livio 1992) show that these are stronger than linear. We therefore chose decreasing intervals with increasing WD mass and adopted four $M_{\rm WD}$-values: 0.65, 1.00, 1.25, and 1.40 $M_\odot$. Earlier studies (Fujimoto 1982b; MacDonald 1983; Iben et al. 1992; Schwartzman et al. 1994) have shown that the WD temperature affects the evolution of a nova outburst in two ways: in cold WDs heat conduction into the core delays the ignition of hydrogen, and thus results in relatively long accretion times (large accreted masses); hot WDs have an outer convective layer that enhances the mixing process between the accreted hydrogen-rich material and heavy elements of the core, thus hastening the occurrence of the TNR. To emphasize these effects, we chose two extreme $T_{\rm WD}$-values—10×10^6 K and 50×10^6 K—as representative of each regime, and one intermediate value, 30×10^6 K. Thus 12 initial models were built for all the parameter combinations, by cooling initially hot models to the desired temperatures. A few pilot runs were required in order to determine the most appropriate (fine) zoning in the outer layers of each WD, those layers that will be affected by diffusion during repeated nova cycles.

The range of possible rates of mass transfer in a close binary system is very wide, extending from $\sim 10^{-6} M_\odot$ yr^{-1}, near the Eddington limit, down to 10^{-11} $M_\odot$ yr^{-1}. Different types of nova outbursts are expected to occur for different accretion rates. However, while the WD mass and core temperature are practically constant for typical outburst timescales, the accretion rate may change during one nova cycle. In fact, according to the hibernation scenario (Shara et al. 1986), it can change appreciably. In the present calculations we assume the accretion rate to be constant, representing an *average* accretion rate. In the case of a variable $\dot{M}$ system, the constant accretion rate assumed should be closer to the lower (quiescence) rate than to the higher one (such as the rate inferred from observations immediately before or following an outburst). Each of the 12 initial models was evolved for accretion rates of 10^{-6}, 10^{-7}, 10^{-8}, 10^{-9}, and 10^{-10} $M_\odot$ yr^{-1}, resulting in 60 parameter combinations. Four additional cases were calculated with $\dot{M} = 10^{-11}$ $M_\odot$ yr^{-1} and $T_{\rm WD} = 50 \times 10^6$ K (the highest temperature) for each WD mass. High WD temperatures and very low accretion rates are expected to maximize the heavy element content of the nova ejecta, while still yielding reasonable recurrence rates (i.e., events that are not too rare to be observed.)

2.3. *Evolutionary Calculations*

We calculated the 64 evolutionary sequences through repeated outburst cycles (between 4 and 15, with an average of $\sim$8), until a regular cyclic pattern was obtained. Only in a few cases (3 or 4) were we compelled to terminate calculations after only two or three cycles. Each sequence took between 25 and 100 CPU hours (depending on the parameters) on a fast HP Apollo workstation. We then selected one cycle in each case as representative and the characteristics of this cycle (given in Tables 1 and 2 below) were used in the analysis of the results. An alternative method would have been to adopt average values—averaged over the repeated regular cycles—for each characteristic. We preferred the first method, as it seems more appropriate for comparison with observations of novae. There are too few well observed novae for deriving average typical characteristics in each nova class, to be compared with average theoretical values. (The latter method, on the other hand, might have given a smoother variation of nova properties with parameter values.) We thus reduced the enormous wealth of data obtained for each evolutionary sequence to a set of values for basic, overall characteristics. Inevitably, a great deal of detailed information about the evolution of each model was discarded in the process.

3. EFFECTS OF THE BASIC PARAMETERS

The evolutionary sequences provide 64 sets of output parameters for a typical cycle, corresponding to the 64 combinations of initial parameters M_{WD}, T_{WD}, and $\dot{M}$. Properties related to the accretion phase and to the onset of an outburst—the accreted mass m_{acc}, the ejected mass m_{ej}, the helium mass fraction in the convective envelope Y_{env} and in the ejecta Y_{ej} (the difference between them indicating the amount of hydrogen burnt during outburst), the heavy element mass fraction of the envelope Z_{env} and of the ejecta Z_{ej} (without distinguishing between abundances of different heavy elements), the maximal temperature attained in the burning shell, at the base of the convective envelope, T_{max} (in units of 10^8 K)—are given in Table 1. Characteristics of the outburst itself—expansion velocities: the maximal velocity v_{max} and its average over the whole mass-loss phase v_{av} (both in km s^{-1}), the maximal luminosity attained L_{max} (in units of 10^4 $L_\odot$), the outburst amplitude A (in magnitudes), and three typical timescales: the duration of the mass-loss phase t_{m-1}, the time of decline of the bolometric luminosity by 3 mag t_{3bol} and the recurrence period of the outbursts, given by $P_{rec} = m_{acc}/\dot{M}$, are given in Table 2.

Some of the listed characteristics require explanation. The determination of the maximal luminosity attained during the evolution of an erupting nova is somewhat problematic. Our aim is to detect the maximum luminosity value that is likely to be observed. Accordingly, we have chosen the maximum luminosity obtained during the mass ejection phase (when the envelope has already expanded), or the plateau luminosity obtained by nonejecting models—phases which are sufficiently long-lived. We would like to mention, however, that the absolute maximum is found to be higher (in some cases almost twice as high) for very short periods of time. Such behavior is usually encountered in nova evolution calculations (J. W. Truran et al. 1994, private communication). Thus, the error in the L_{max} determination can be as large as -0.75 mag. Nevertheless, our calculations very seldom yield peak luminosities in excess of 10 times the nominal (electron scattering opacity) Eddington luminosity, as is sometimes observed (e.g., V1500 Cyg; Lance, McCall, & Uomoto 1988). The observed luminosity during the mass loss phase includes in addition to the radiative diffusion term L (the photon flux in the fluid frame) an advective term $L_{adv} = 4\dot{m}P_{rad}/\rho$ (Cassinelli & Castor 1973), but the added term is very small. It should, perhaps be noted that the highest luminosities are obtained for cold WDs accreting at a slow rate; among those, the WDs of *lowest* mass achieve the highest luminosity.

The amplitude of the outburst A (in mag) is the ratio of the maximum luminosity L_{max} to the quiescence luminosity, which is essentially L_{acc} given in equation (4). For hot WDs accreting at low rates L_{acc} may be lower than the intrinsic WD luminosity. In such cases the minimum luminosity is $\sim L_{WD}$. The amplitude given in Table 2 should be regarded as an upper limit to the actual observed amplitude, which is usually measured from the minimum that occurs a relatively short time after outburst, when the mass transfer rate is still slowly declining (Vogt 1990; Duerbeck 1992).

The duration of mass loss provides a lower limit to the observed time of decline of the visual (or blue) magnitude by 3 mag, known as t_3. When mass loss ceases, the star starts contracting and the emitted radiation shifts rapidly toward the blue. However, the central star is seen through the expanding envelope and the observed shift to the blue may be delayed until the envelope becomes transparent. Nevertheless, since the ejected mass in a nova event is small and thus becomes quickly diluted, t_{m-1} should be considered a reasonable lower limit to the decline time by a few magnitudes, such as t_3. The largest differences between t_{m-1} and t_3 are expected to occur for the lowest t_{m-1}, when the duration of mass loss is comparable to the contraction time of the envelope that defines t_3. Obviously, t_{3bol} represents an upper limit to t_3, but this is not very significant, since the bolometric luminosity may remain high long after the decline of the visual magnitude caused by the contraction of the central star. Indeed, when observations of the later stages of nova evolution are available, they show a rise in the UV and the IR (due to dust formation) after the visual decline.

Finally, the recurrence period, calculated as $m_{acc}/\dot{M}$, represents the duration of the low-luminosity state of a nova cycle, which is usually much longer than the high-luminosity state, $P_{rec} \gg t_{3bol}$. Strictly, however, the recurrence period should be taken as the sum of P_{rec} and t_{3bol}.

The following analysis will be entirely based on the data given in these tables.

3.1. *Ranges of Variation of Different Properties*

The range of variation of properties which are of interest, either observationally or theoretically, is given in Table 3, where maximum and minimum values are listed, together with the parameters for which they were obtained. The remnant mass of the convective envelope, which is burnt into helium following an outburst, is denoted m_{rem}; it represents the difference between the mass of the convective envelope—extending from the base of the burning shell to the surface of the star— at the peak of the TNR, and the ejected mass. The range of variation of nova characteristics is also illustrated in Figures 1*a*–1*d*, where m_{acc}, T_{max}, log L_{max}, and log t_{3bol} are plotted versus M_{WD}, and in Figures 2*a* and 2*b*, where Z_{ej} and A are plotted versus $\dot{M}$. The obvious conclusion is that novae represent a three parameter family of events and all parameters affect all properties to a larger or lesser extent. This basic conclusion and some of the above relations were discussed in more detail by Prialnik (1993) and by Schwartzman et al. (1994), based on many different previous calculations. Another important conclusion is that the theoretical results cover the entire ranges directly observed or inferred from observations, with very few exceptions (e.g., the currently adopted $Z_{ej} = 0.86$ value for Nova V1370 Aql, or the huge amplitude of over 19 mag of Nova V1500 Gyg—which could still be obtained for a cold WD, accreting at a very low rate, $\dot{M} \leq 10^{-11}\ M_\odot\ yr^{-1}$.)

3.2. *Contours*

In order to determine the effect of parameters on nova outburst properties we have divided the models into three groups, according to the three initial WD temperatures: cold, moderate and hot. Interpolating between the results obtained in each group, we derive the trend of change of different properties with the other two parameters, by drawing contours of constant values in the ($\dot{M}$, M_{WD}) plane.

Such contours are given in Figures 3–5, each showing three different properties. Properties have been grouped according to the parameter that is expected to affect them most. Thus in Figure 3 we show log m_{acc}, log t_{3bol}, and log L_{max}, all of which are analytically regarded, in the simplest approximation, as functions of M_{WD} only (Fujimoto 1982a; Shara 1981; Livio 1992). We note, however, that they are significantly affected by the other two parameters as well. We shall bear this in mind

TABLE 1

CHARACTERISTICS OF THE NOVA ENVELOPE

M_{WD}	T_{WD}	$\dot{M}$	m_{acc}	m_{ej}	Y_{env}	Y_{ej}	Z_{env}	Z_{ej}	$T_{8,max}$
0.65.....	10.	−6.	8.35E−06	...	0.283	...	2.08E−02	...	0.81
0.65.....	10.	−7.	2.45E−05	...	0.343	...	2.03E−02	...	1.10
0.65.....	10.	−8.	1.01E−04	1.03E−04	0.375	0.387	2.07E−02	2.15E−02	1.34
0.65.....	10.	−9.	1.61E−04	1.63E−04	0.254	0.265	1.20E−01	1.35E−01	1.39
0.65.....	10.	−10.	2.55E−04	2.76E−04	0.241	0.250	1.64E−01	1.79E−01	1.67
0.65.....	30.	−6.	8.63E−06	...	0.283	...	2.08E−02	...	0.80
0.65.....	30.	−7.	2.54E−05	...	0.369	...	2.03E−02	...	1.09
0.65.....	30.	−8.	1.02E−04	1.01E−04	0.369	0.380	2.08E−02	2.14E−02	1.22
0.65.....	30.	−9.	1.11E−04	1.21E−04	0.288	0.296	1.04E−01	1.10E−01	1.21
0.65.....	30.	−10.	9.55E−05	1.21E−04	0.246	0.249	2.25E−01	2.37E−01	1.24
0.65.....	50.	−6.	8.94E−06	...	0.286	...	2.06E−02	...	0.80
0.65.....	50.	−7.	2.66E−05	...	0.350	...	2.03E−02	...	0.97
0.65.....	50.	−8.	1.06E−04	9.88E−05	0.367	0.377	2.07E−02	2.12E−02	1.31
0.65.....	50.	−9.	7.41E−05	9.16E−05	0.256	0.258	2.10E−01	2.21E−01	1.16
0.65.....	50.	−10.	5.23E−05	6.72E−05	0.255	0.257	2.44E−01	2.55E−01	1.20
0.65.....	50.	−11.	3.86E−05	5.36E−05	0.248	0.255	3.10E−01	3.16E−01	1.09
1.00.....	10.	−6.	2.05E−06	...	0.326	...	2.04E−02	...	1.05
1.00.....	10.	−7.	8.96E−06	7.21E−06	0.342	0.419	2.10E−02	2.23E−02	1.41
1.00.....	10.	−8.	2.06E−05	2.22E−05	0.304	0.331	9.37E−02	1.00E−01	1.59
1.00.....	10.	−9.	4.66E−05	5.18E−05	0.268	0.297	1.20E−01	1.27E−01	1.86
1.00.....	10.	−10.	8.40E−05	9.72E−05	0.243	0.274	1.55E−01	1.62E−01	2.10
1.00.....	30.	−6.	2.10E−06	...	0.316	...	2.04E−02	...	1.04
1.00.....	30.	−7.	8.74E−06	5.74E−06	0.328	0.354	2.08E−02	2.15E−02	1.34
1.00.....	30.	−8.	2.03E−05	2.19E−05	0.304	0.330	9.51E−02	1.01E−01	1.57
1.00.....	30.	−9.	2.70E−05	3.10E−05	0.269	0.294	1.49E−01	1.59E−01	1.68
1.00.....	30.	−10.	2.10E−05	2.70E−05	0.238	0.259	2.41E−01	2.56E−01	1.66
1.00.....	50.	−6.	2.15E−06	...	0.322	...	2.03E−02	...	1.03
1.00.....	50.	−7.	8.30E−06	5.05E−06	0.324	0.347	2.07E−02	2.10E−02	1.39
1.00.....	50.	−8.	2.27E−05	2.27E−05	0.363	0.389	2.27E−02	2.72E−02	1.58
1.00.....	50.	−9.	1.62E−05	1.94E−05	0.272	0.293	1.84E−01	1.96E−01	1.53
1.00.....	50.	−10.	1.09E−05	1.42E−05	0.262	0.281	2.49E−01	2.64E−01	1.46
1.00.....	50.	−11.	7.94E−06	1.19E−05	0.222	0.245	3.71E−01	3.79E−01	1.43
1.25.....	10.	−6.	4.14E−07	...	0.318	...	2.04E−02	...	1.27
1.25.....	10.	−7.	1.92E−06	1.62E−06	0.319	0.374	2.17E−02	2.63E−02	1.62
1.25.....	10.	−8.	3.67E−06	3.91E−06	0.298	0.364	8.34E−02	8.76E−02	1.90
1.25.....	10.	−9.	9.27E−06	1.06E−05	0.256	0.334	1.42E−01	1.41E−01	2.33
1.25.....	10.	−10.	1.91E−05	2.18E−05	0.247	0.322	1.41E−01	1.56E−01	2.70
1.25.....	30.	−6.	3.82E−07	...	0.330	...	2.03E−02	...	1.23
1.25.....	30.	−7.	1.96E−06	1.86E−06	0.384	0.438	2.24E−02	2.73E−02	1.67
1.25.....	30.	−8.	3.84E−06	4.16E−06	0.303	0.367	9.96E−02	1.04E−01	1.92
1.25.....	30.	−9.	5.22E−06	5.86E−06	0.273	0.340	1.31E−01	1.36E−01	2.05
1.25.....	30.	−10.	4.35E−06	5.55E−06	0.242	0.306	2.38E−01	2.48E−01	2.05
1.25.....	50.	−6.	4.16E−07	...	0.315	...	2.05E−02	...	1.26
1.25.....	50.	−7.	1.96E−06	1.78E−06	0.337	0.422	2.18E−02	2.69E−02	1.67
1.25.....	50.	−8.	3.69E−06	4.01E−06	0.303	0.366	1.02E−01	1.07E−01	1.89
1.25.....	50.	−9.	3.18E−06	3.58E−06	0.280	0.342	1.50E−01	1.58E−01	1.86
1.25.....	50.	−10.	2.14E−06	2.78E−06	0.258	0.313	2.52E−01	2.66E−01	1.78
1.25.....	50.	−11.	1.62E−06	2.51E−06	0.221	0.282	3.93E−01	3.97E−01	1.76
1.40.....	10.	−6.	1.81E−08	...	0.337	...	2.13E−02	...	1.64
1.40.....	10.	−7.	7.71E−08	5.31E−08	0.309	0.460	2.18E−02	2.72E−02	2.09
1.40.....	10.	−8.	1.64E−07	1.83E−07	0.298	0.500	1.28E−01	1.28E−01	2.52
1.40.....	10.	−9.	4.12E−07	4.74E−07	0.262	0.473	1.54E−01	1.52E−01	3.07
1.40.....	10.	−10.	5.90E−07	6.90E−07	0.254	0.407	1.59E−01	2.25E−01	3.62
1.40.....	30.	−6.	1.78E−08	...	0.347	...	2.08E−02	...	1.62
1.40.....	30.	−7.	7.94E−08	5.54E−08	0.307	0.457	2.17E−02	2.71E−02	2.10
1.40.....	30.	−8.	2.02E−07	2.02E−07	0.360	0.541	2.42E−02	3.39E−02	2.51
1.40.....	30.	−9.	2.64E−07	3.02E−07	0.282	0.489	1.49E−01	1.50E−01	2.81
1.40.....	30.	−10.	2.11E−07	2.68E−07	0.251	0.464	2.34E−01	2.33E−01	2.76
1.40.....	50.	−6.	1.80E−08	...	0.335	...	2.14E−02	...	1.62
1.40.....	50.	−7.	8.09E−08	5.69E−08	0.309	0.477	2.18E−02	2.77E−02	2.07
1.40.....	50.	−8.	2.02E−07	2.02E−07	0.360	0.539	2.41E−02	3.36E−02	2.48
1.40.....	50.	−9.	1.90E−07	2.18E−07	0.293	0.495	1.54E−01	1.54E−01	2.60
1.40.....	50.	−10.	1.21E−07	1.64E−07	0.261	0.468	2.85E−01	2.84E−01	2.48
1.40.....	50.	−11.	6.83E−08	1.25E−07	0.222	0.423	4.75E−01	4.73E−01	2.40

TABLE 2

CHARACTERISTICS OF THE OUTBURST

M_{WD}	T_{WD}	$\dot{M}$	v_{max}	v_{av}	$L_{4,max}$	A	t_{m-1}(days)	t_{3bol}(days)	P_{rec}(yr)	Type
0.65.....	10.	−6.	...	...	1.18	4.2	...	2.65E+04	8.35E+00	
0.65.....	10.	−7.	...	...	1.48	6.9	...	5.67E+04	2.45E+02	SymN
0.65.....	10.	−8.	156	122	1.52	9.4	1.17E+03	2.93E+04	1.01E+04	SymN
0.65.....	10.	−9.	2590	2150	4.76	13.2	2.64E+02	3.83E+04	1.61E+05	NS
0.65.....	10.	−10.	4210	2650	13.7	16.8	1.17E+02	3.23E+04	2.55E+06	NS
0.65.....	30.	−6.	...	...	1.17	4.1	...	2.82E+04	8.63E+00	
0.65.....	30.	−7.	...	...	1.49	6.9	...	6.01E+04	2.54E+02	SymN
0.65.....	30.	−8.	139	125	1.58	9.5	1.22E+03	3.22E+04	1.02E+04	SymN
0.65.....	30.	−9.	210	156	1.65	12.0	6.79E+02	1.27E+04	1.11E+05	NVS
0.65.....	30.	−10.	316	195	7.96	16.2	4.83E+02	8.38E+03	9.55E+05	NVS
0.65.....	50.	−6.	...	...	1.14	4.1	...	2.98E+04	8.94E+00	
0.65.....	50.	−7.	...	...	1.42	6.9	...	6.44E+04	2.66E+02	SymN
0.65.....	50.	−8.	159	130	1.60	9.5	1.17E+03	4.38E+04	1.06E+04	SymN
0.65.....	50.	−9.	340	240	1.73	12.0	4.39E+02	7.91E+03	7.41E+04	NVS
0.65.....	50.	−10.	369	208	1.91	13.6	3.59E+02	7.51E+03	5.22E+05	NVS
0.65.....	50.	−11.	416	179	2.17	13.7	3.56E+02	6.54E+03	3.86E+06	NVS
1.00.....	10.	−6.	...	...	2.96	4.2	...	2.43E+03	2.05E+00	
1.00.....	10.	−7.	265	240	3.45	6.9	2.10E+02	2.72E+03	8.96E+01	RN
1.00.....	10.	−8.	351	271	3.26	9.4	1.27E+02	1.35E+03	2.06E+03	NS
1.00.....	10.	−9.	525	256	3.88	12.0	9.35E+01	1.13E+03	4.66E+04	NM
1.00.....	10.	−10.	1920	1180	11.3	15.7	3.36E+01	1.28E+02	8.40E+05	NF
1.00.....	30.	−6.	...	...	2.96	4.2	...	2.53E+03	2.10E+00	
1.00.....	30.	−7.	267	237	3.26	6.9	2.17E+02	3.35E+03	8.74E+01	RN
1.00.....	30.	−8.	355	274	3.28	9.4	1.57E+02	1.32E+03	2.03E+03	NS
1.00.....	30.	−9.	475	324	3.61	12.0	1.41E+02	1.02E+03	2.70E+04	NS
1.00.....	30.	−10.	512	344	3.55	14.4	1.18E+02	7.08E+02	2.10E+05	NS
1.00.....	50.	−6.	...	...	2.97	4.3	...	2.60E+03	2.15E+00	
1.00.....	50.	−7.	300	239	3.21	6.8	2.53E+02	3.56E+03	8.30E+01	RN
1.00.....	50.	−8.	360	272	3.60	9.5	2.40E+02	2.51E+03	2.27E+03	NS
1.00.....	50.	−9.	400	328	3.57	12.0	1.43E+02	9.50E+02	1.62E+04	NS
1.00.....	50.	−10.	384	302	3.71	14.0	9.14E+01	8.48E+02	1.09E+05	NM
1.00.....	50.	−11.	680	471	4.89	14.3	1.22E+02	5.28E+02	7.94E+05	NS
1.25.....	10.	−6.	...	...	4.57	4.0	...	3.11E+02	4.14E−01	
1.25.....	10.	−7.	414	346	4.84	6.5	6.51E+01	2.59E+02	1.92E+01	RN
1.25.....	10.	−8.	1110	568	6.38	9.3	2.02E+01	1.31E+02	3.67E+02	NF
1.25.....	10.	−9.	1480	413	6.67	11.9	9.56E+00	9.78E+01	9.27E+03	NVF
1.25.....	10.	−10.	2230	1940	7.14	14.5	2.43E+01	1.38E+02	1.91E+05	NVF
1.25.....	30.	−6.	...	...	4.52	4.0	...	2.46E+02	3.82E−01	
1.25.....	30.	−7.	474	373	4.77	6.5	6.01E+01	2.36E+02	1.96E+01	RN
1.25.....	30.	−8.	734	531	4.78	9.0	3.22E+01	1.62E+02	3.84E+02	NF
1.25.....	30.	−9.	1030	589	5.14	11.6	3.14E+01	1.25E+02	5.22E+03	NF
1.25.....	30.	−10.	1230	678	6.04	14.3	2.20E+01	1.13E+02	4.35E+04	NF
1.25.....	50.	−6.	...	...	4.53	4.0	...	3.15E+02	4.16E−01	
1.25.....	50.	−7.	436	355	4.75	6.5	4.75E+01	2.55E+02	1.96E+01	RN
1.25.....	50.	−8.	807	533	4.61	9.0	4.30E+01	1.58E+02	3.69E+02	NM
1.25.....	50.	−9.	689	485	4.72	11.5	2.47E+01	1.54E+02	3.18E+03	NF
1.25.....	50.	−10.	921	542	4.97	14.1	3.04E+01	1.01E+02	2.14E+04	NF
1.25.....	50.	−11.	889	658	5.45	14.3	2.59E+01	7.77E+01	1.62E+05	NF
1.40.....	10.	−6.	...	...	5.92	3.4	...	1.08E+01	1.81E−02	
1.40.....	10.	−7.	1410	681	6.03	5.9	4.13E+00	1.19E+01	7.71E−01	
1.40.....	10.	−8.	3060	1160	9.27	8.8	1.57E+00	5.02E+00	1.64E+01	RN
1.40.....	10.	−9.	2850	1020	9.23	11.3	1.39E+00	4.31E+00	4.12E+02	NVF
1.40.....	10.	−10.	5270	2020	10.1	13.9	6.78E−01	5.45E+00	5.90E+03	NVF
1.40.....	30.	−6.	...	...	5.86	3.3	...	1.11E+01	1.78E−02	
1.40.....	30.	−7.	1160	723	5.99	5.9	3.64E+00	1.19E+01	7.94E−01	
1.40.....	30.	−8.	1760	840	6.14	8.4	4.63E+00	9.35E+00	2.02E+01	RN
1.40.....	30.	−9.	3760	1800	6.98	11.0	1.29E+00	6.17E+00	2.64E+02	NVF
1.40.....	30.	−10.	4490	2120	7.67	13.6	1.50E+00	4.20E+00	2.11E+03	NVF
1.40.....	50.	−6.	...	...	5.85	3.3	...	1.11E+01	1.80E−02	
1.40.....	50.	−7.	1360	812	6.01	5.8	4.24E+00	1.25E+01	8.09E−01	
1.40.....	50.	−8.	1540	833	6.46	8.4	4.80E+00	9.49E+00	2.02E+01	RN
1.40.....	50.	−9.	3740	1580	7.18	11.1	1.76E+00	6.03E+00	1.90E+02	NVF
1.40.....	50.	−10.	4350	1870	7.67	13.6	1.17E+00	4.71E+00	1.21E+03	NVF
1.40.....	50.	−11.	3630	1900	7.74	14.8	1.67E+00	3.45E+00	6.83E+03	NVF

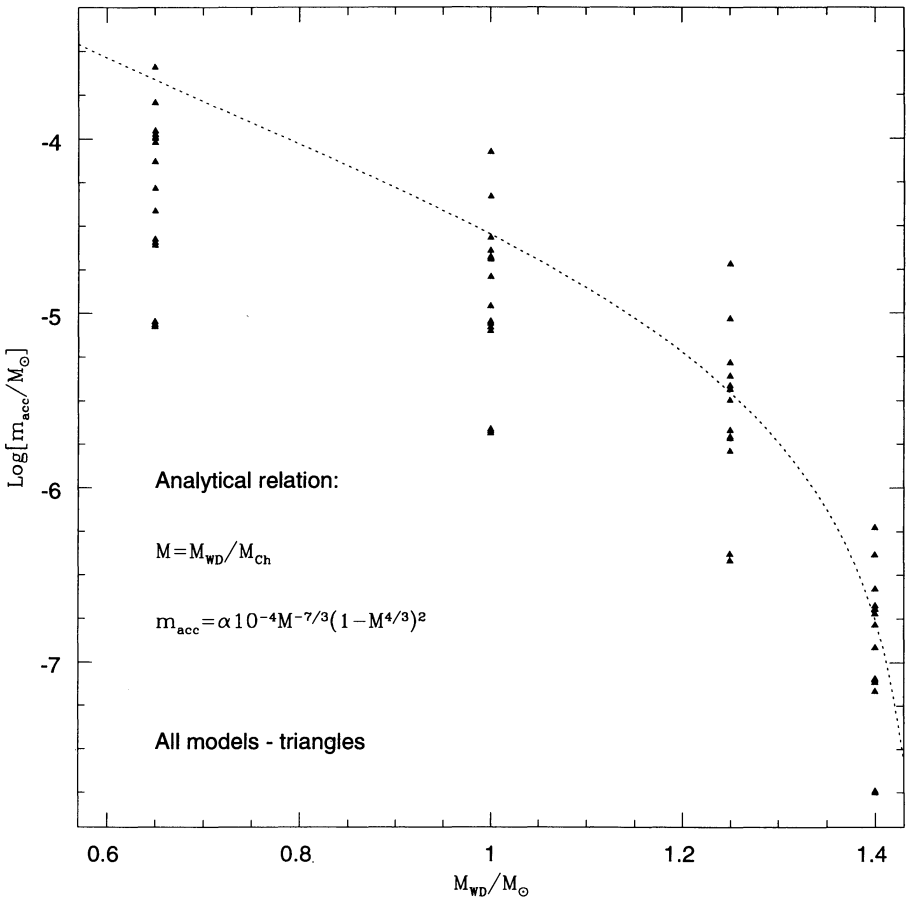

FIG. 1*a*

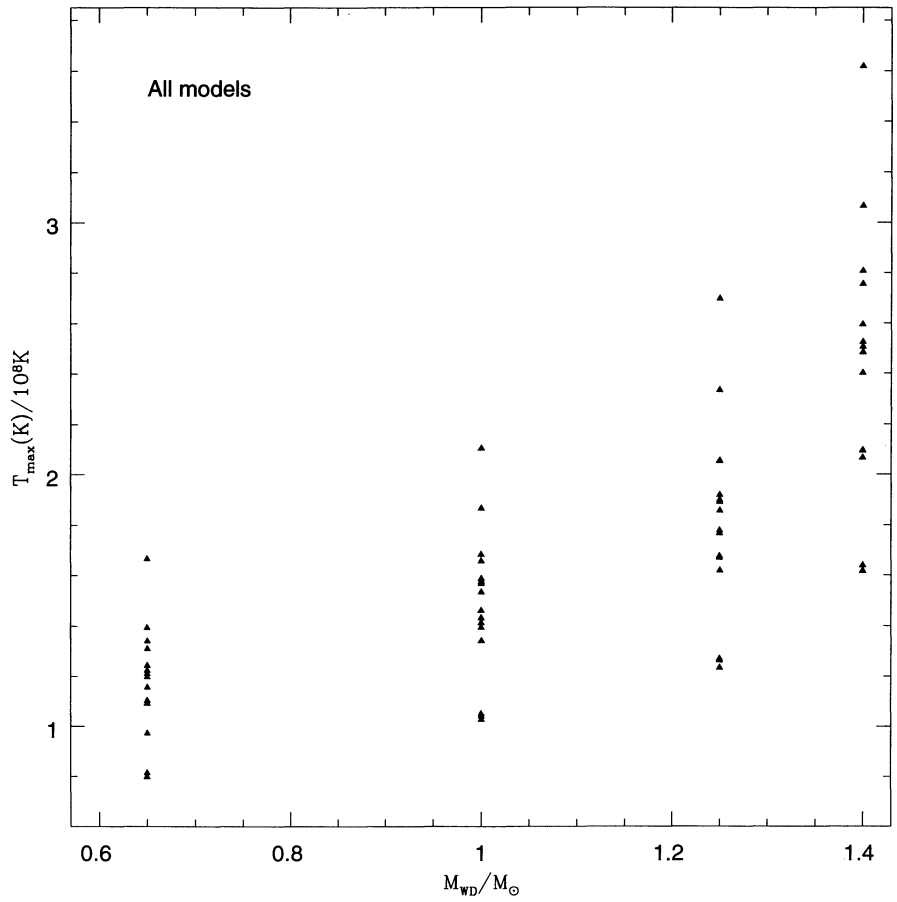

FIG. 1*b*

FIG. 1.—(*a*) Accreted mass—on a logarithmic scale—as a function of the WD mass for all models. The vertical spread in calculated points is due to the effect of different T_{WD} and $\dot{M}$. The analytical relation is shown by a dotted line; α is a fudge factor of order unity. (*b*) Peak temperature attained at outburst (in units of 10^8 K) as a function of the WD mass for all models. (*c*) Maximal bolometric luminosity (see comments in text)—on a logarithmic scale—as a function of the WD mass for all models. The (nominal) Eddington luminosity, calculated assuming a constant electron-scattering opacity, is given by the dotted line. (*d*) Time of decline of the bolometric luminosity by 3 magnitudes as a function of the WD mass for all models.

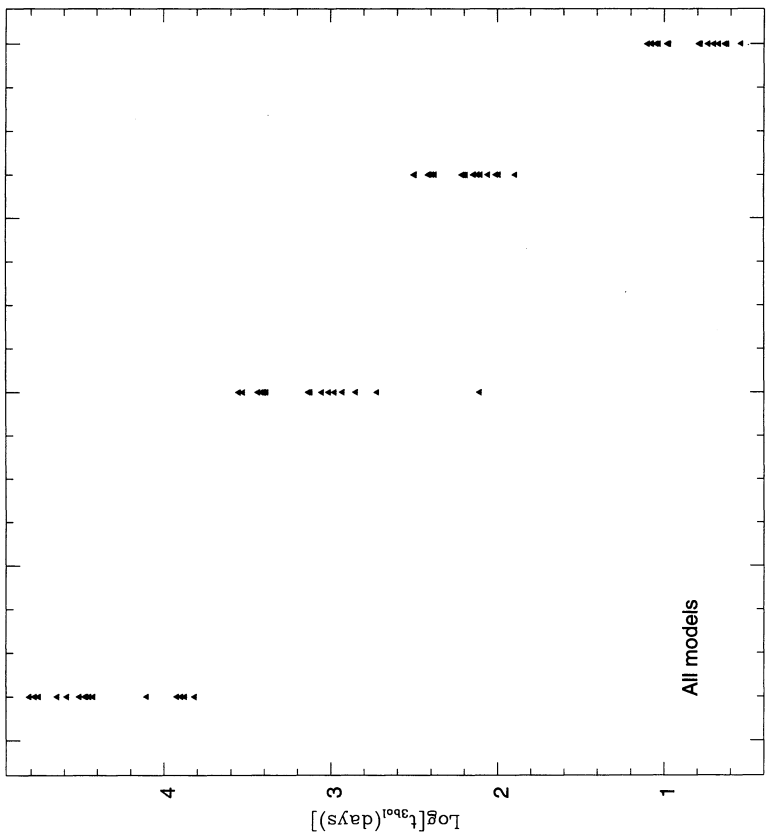

FIG. 1*d*

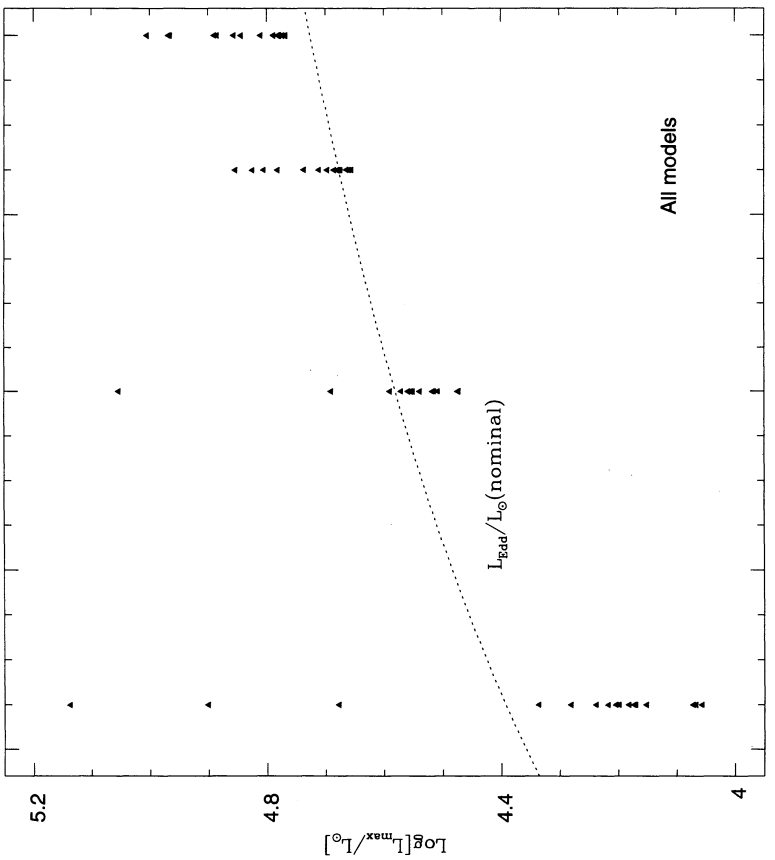

FIG. 1*c*

1995ApJ...445..789P

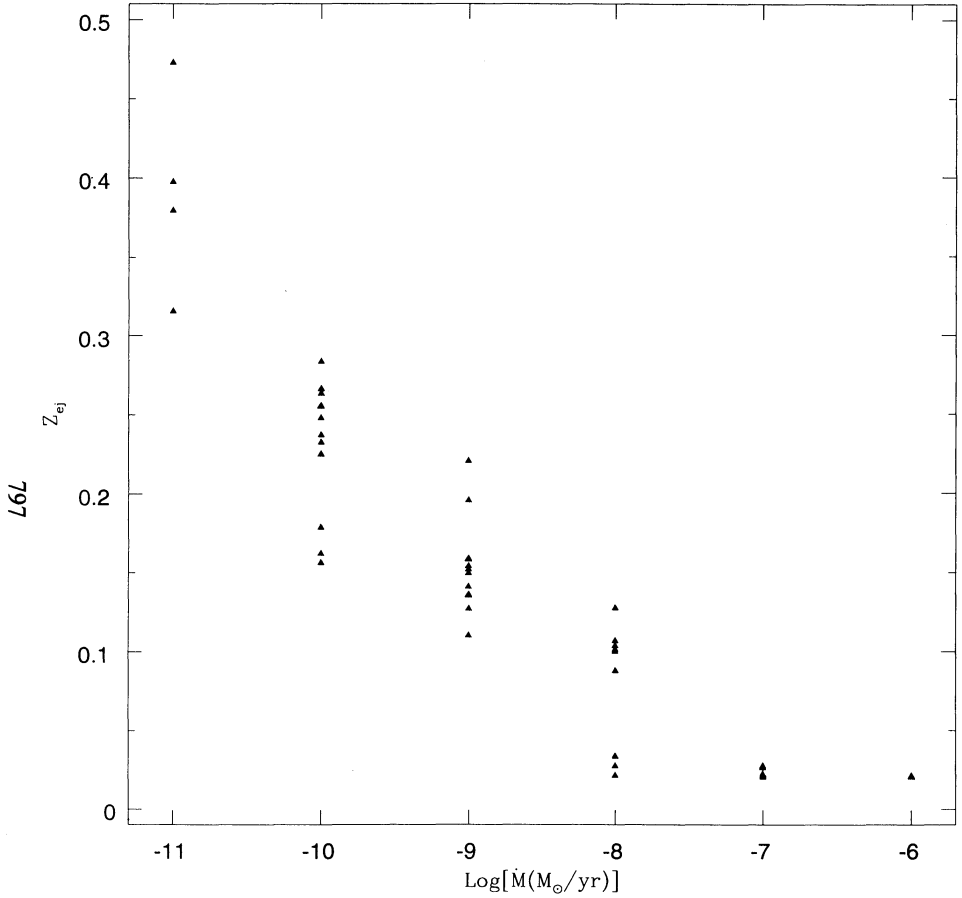

FIG. 2a

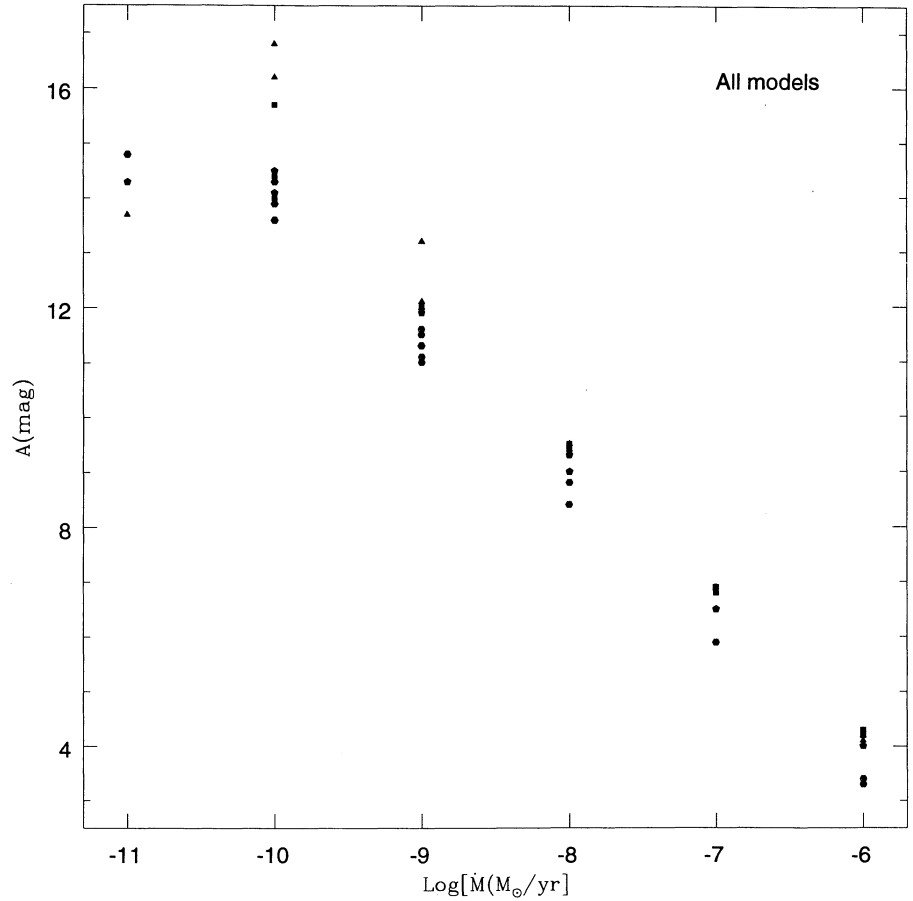

FIG. 2b

FIG. 2.—(*a*) Average mass fraction of heavy elements in the ejecta (or in the convective envelope of nonejecting models) as a function of accretion rate—on a logarithmic scale. (*b*) Outburst amplitude (in magnitudes) as a function of accretion rate. The WD mass is indicated by different symbols: (*triangles*) 0.65 $M_\odot$; (*squares*) 1 $M_\odot$; (*pentagons*) 1.25 $M_\odot$; (*hexagons*) 1.4 $M_\odot$.

TABLE 3

MAXIMUM AND MINIMUM VALUES OF NOVA CHARACTERISTICS

Characteristic	MAX	M_{WD}	T_{WD}	$\dot{M}$	MIN	M_{WD}	T_{WD}	$\dot{M}$
$T_{max}(10^8$ K)	3.619	1.40	10.	−10.	0.798	0.65	50.	−6.
$m_{acc}/M_\odot$	2.554(−4)	0.65	10.	−10.	1.776(−8)	1.40	30.	−6.
$m_{ej}/M_\odot$	2.762(−4)	0.65	10.	−10.	5.305(−8)	1.40	10.	−7.
$m_{rem}/M_\odot$	2.658(−5)	0.65	50.	−7.	8.565(−10)	1.4	50.	−8.
Z_{ej}	0.473	1.40	50.	−11.	0.021	1.00	50.	−7.
Y_{ej}	0.541	1.40	30.	−8.	0.245	1.00	50.	−11.
X_{ej}	0.632	1.00	50.	−7.	0.104	1.40	50.	−11.
t_{3bol}	176 yr	0.65	50.	−7.	3.45 days	1.40	50.	−11.
t_{m-1}	3.33 yr	0.65	30.	−8.	0.68 days	1.40	10.	−10.
$M_{bol,max}$	−8.022	0.65	10.	−10.	−5.322	0.65	50.	−6.
A(mag)	16.8	0.65	10.	−10.	3.3	1.40	50.	−6.
v_{av}(km s^{-1})	2650	0.65	10.	−10.	122	0.65	10.	−8.
v_{max}(km s^{-1})	5270	1.40	10.	−10.	139	0.65	30.	−8.

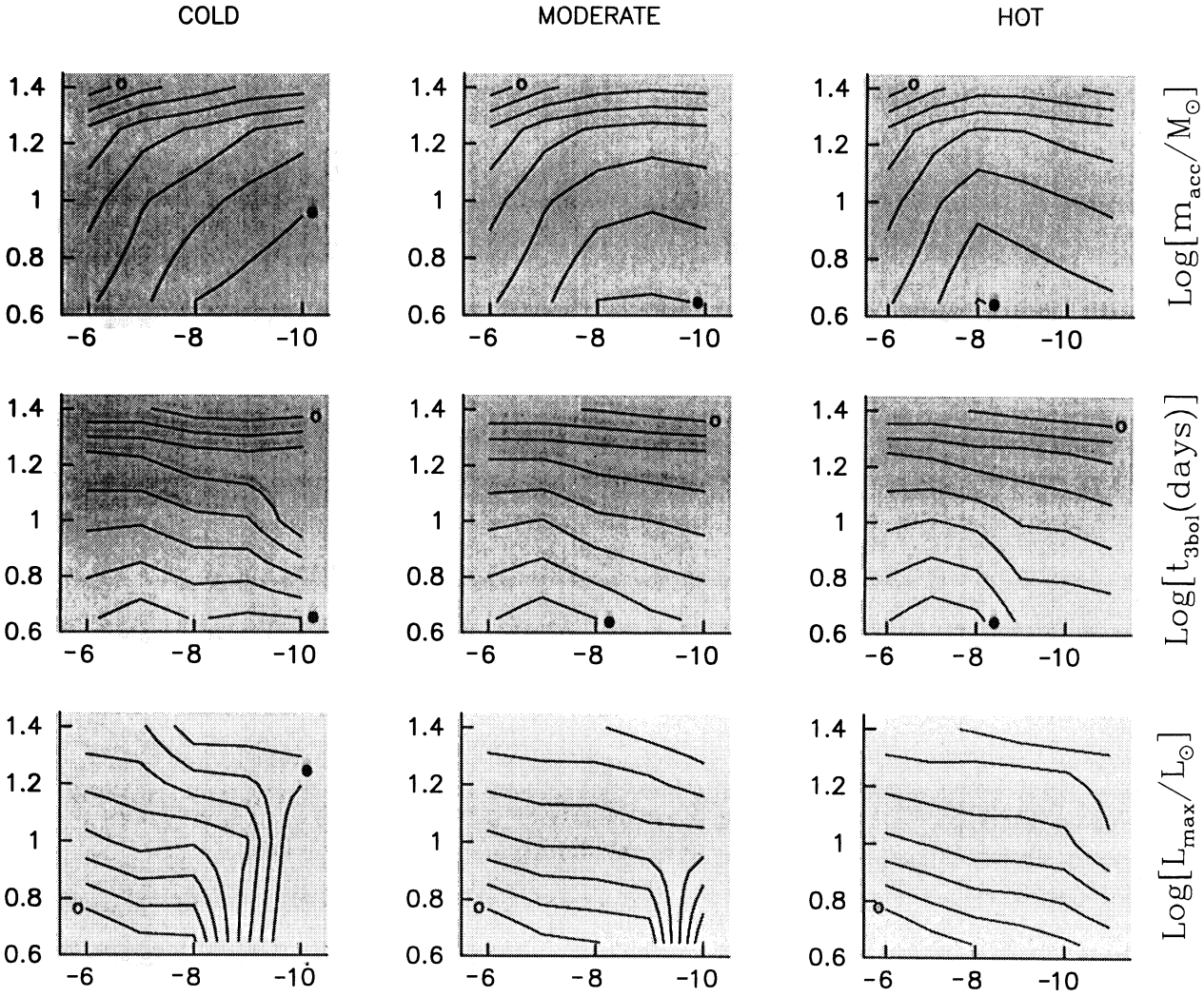

FIG. 3.—Contours of constant accreted masses m_{acc} (*upper panels*), times of decline of the bolometric luminosity t_{3bol} (*middle panels*) and maximal bolometric luminosities L_{max} (*lower panels*) in the ($\dot{M}$, M_{WD}) plane for each of the three WD temperatures: 10^7 K (cold), 3×10^7 K (moderate) and 5×10^7 K (hot). The eight (logarithmic) contour values are equally spaced, from the minimum marked by an open circle, to a maximum marked by a filled circle. Accreted masses start from log $m_{acc} = -7.5$ with increments of 0.5; decline times (in days) start from log $t_{3bol} = 1$ with increments of 0.5 and luminosities start from log $L_{max} = 4.2$ with increments of 0.1.

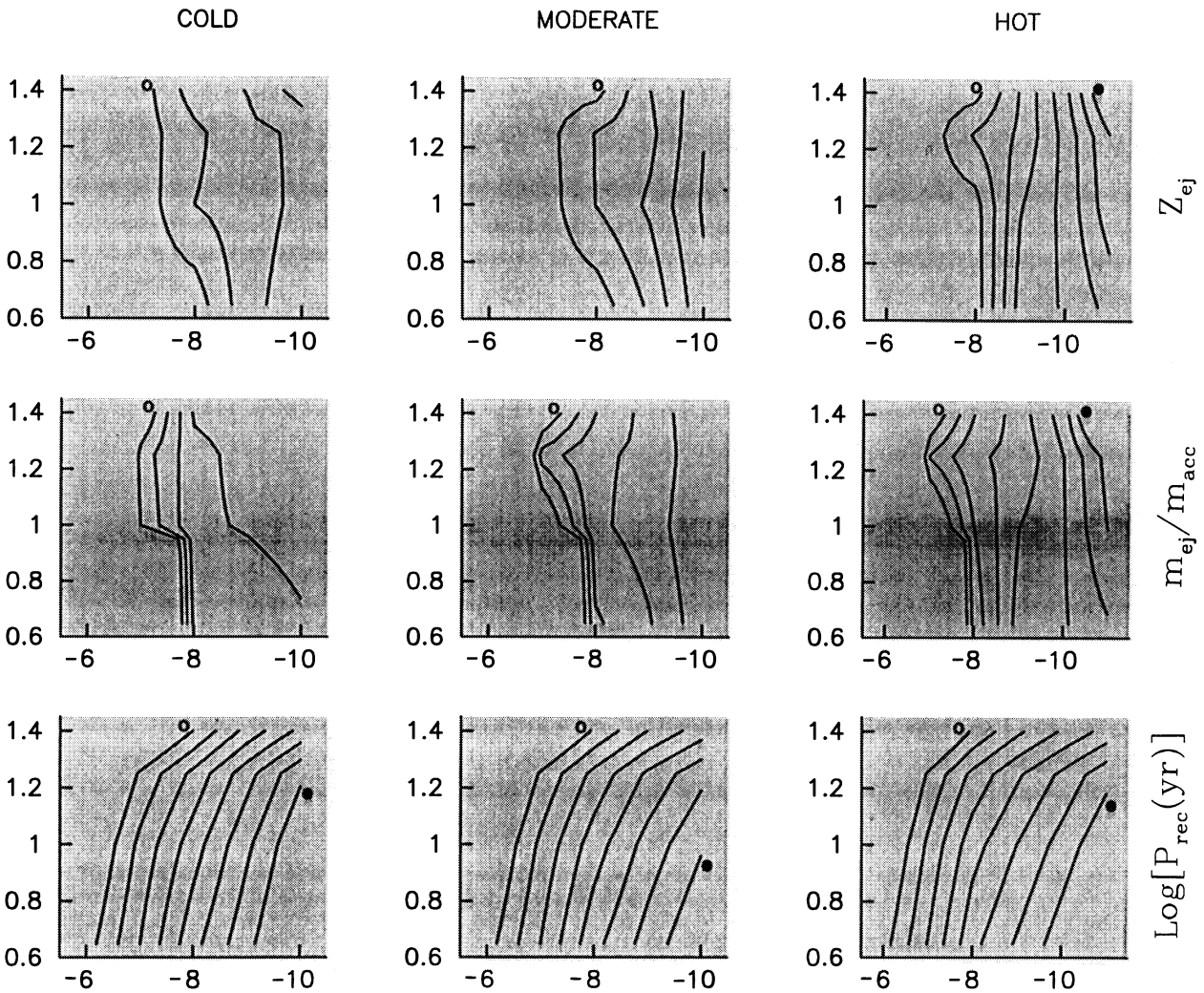

FIG. 4.—Contours of constant heavy element mass fractions Z_{ej} (*upper panels*), ratios of ejected to accreted mass m_{ej}/m_{acc} (*middle panels*) and outburst recurrence periods log P_{rec} (*lower panels*) in the ($\dot{M}$, M_{WD}) plane for each of the three WD temperatures: 10^7 K (cold), 3×10^7 K (moderate) and 5×10^7 K (hot). The eight contour values are equally spaced, from the minimum marked by an open circle, to a maximum marked by a filled circle. Mass fractions start from $Z_{ej} = 0.05$ with increments of 0.05; ejected to accreted mass ratios start from $m_{ej}/m_{acc} = 0.8$ with increments of 0.1 and recurrence periods (in years) start from log $P_{rec} = 1.2$ with increments of 0.6.

when we discuss, in the next section, the famous (M_B, t_3) relationship. In Figure 4 parameters that are mostly affected by $\dot{M}$ are shown: Z_{ej}, the ratio of ejected to accreted matter, and log P_{rec}. We note the strong effect of the WD's temperature on Z_{ej} (mentioned in § 2.2) and also on the ratio m_{ej}/m_{acc}. The recurrence period, on the other hand, is almost unaffected by T_{WD}. In Figure 5 a more erratic behavior is illustrated; all three properties shown, T_{max}, v_{max}, and Y_{ej}, are strongly influenced by all three parameters. Note the dominant effect of M_{WD} at high masses, which obliterates the effect of the other parameters: curves tend to become parallel to the $\dot{M}$ axis in all temperature regimes.

3.3. *General Results Regarding Nova Evolution*

A very important problem related to the nova theory is to determine the conditions required for the WD to increase its mass at each cycle ($\dot{M}_{WD} > 0$). The average long-term rate of change of the WD mass is given by

$$\dot{M}_{WD} = (m_{acc} - m_{ej})/P_{rec} = \dot{M}(1 - m_{ej}/m_{acc}) .$$

The extent and location of the subspace of parameter space leading to such growth will determine the viability of the accretion scenario (as opposed to the WD mergers) for Type Ia supernova progenitors (Livio 1994; Della Valle & Livio 1994). The ratio of ejected to accreted mass is plotted in Figure 6 versus $\dot{M}$. The situation seems to be rather simple: for $\dot{M} \geq 10^{-7}\ M_\odot\ yr^{-1}$, the WD will grow in mass, regardless of its mass and temperature, whereas for $\dot{M} \leq 10^{-9}\ M_\odot\ yr^{-1}$, it will always lose mass. Only in a relatively narrow range of accretion rates, around $10^{-8}\ M_\odot\ yr^{-1}$, will the WD's fate be determined by its temperature, hot WDs losing less material than cold ones. For $T_{WD} = 10 \times 10^6$ K, all WDs lose mass when accreting at $10^{-8}\ M_\odot\ yr^{-1}$. At higher temperatures, low-mass WDs gain mass, while massive ones lose mass. Thus, under these conditions, if the mass transfer rate remains constant (or increases), the WD would not be able to increase its mass up to the Chandrasekhar limit. It should perhaps be noted that the foregoing considerations did not take into account any possible mass loss due to dynamical friction between the secondary star and the expanding envelope.

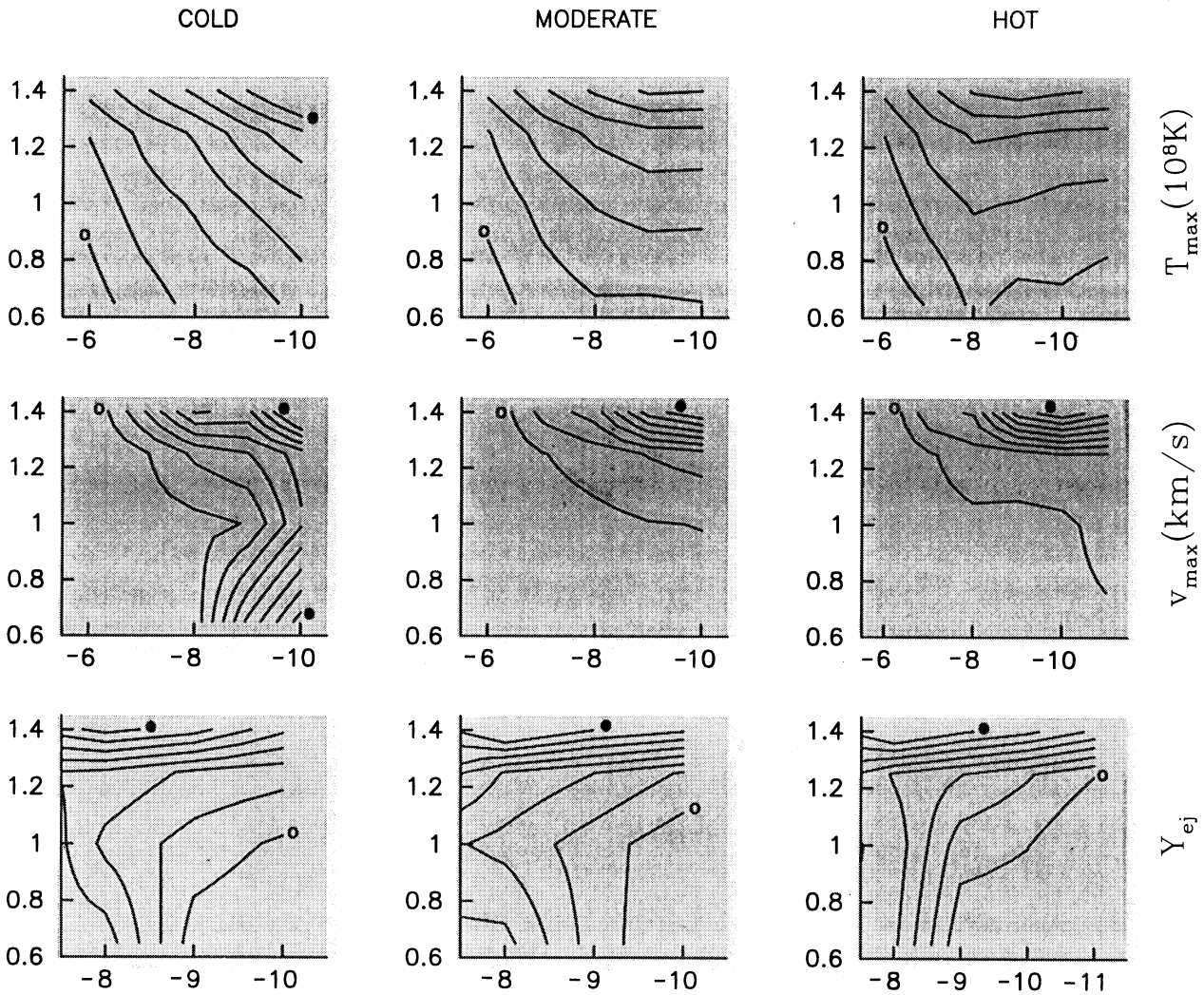

FIG. 5.—Contours of constant peak temperatures T_{max} (*upper panels*), maximal velocities v_{max} (*middle panels*) and helium mass fractions in the ejecta (*lower panels*) in the ($\dot{M}$, M_{WD}) plane for each of the three WD temperatures: 10^7 K (cold), 3×10^7 K (moderate) and 5×10^7 K (hot). The eight contour values are equally spaced, from the minimum marked by an open circle, to a maximum marked by a filled circle. Peak temperatures (in units of 10^8 K) start from $T_{max} = 0.95$ with increments of 0.3; velocities (in km s^{-1}) start from $v_{max} = 500$ with increments of 500 and helium mass fractions start from $Y_{ej} = 0.28$ with increments of 0.03.

We find a strong correlation between t_{m-1} and t_{3bol}, as illustrated in Figure 7; the latter is on the average about an order of magnitude longer than the former (the ratio t_{3bol}/t_{m-1} varies between 3 and 40). This result may be verified by observations. Recent evidence for a correlation between the UV flux decline time and t_3 has, in fact, been deduced from *IUE* observations (R. Gonzalez-Riestra 1994, private communication). Since the effective temperature of the nova rises to $\sim 10^5$ K after the mass-loss phase, the UV decline time is well approximated by t_{3bol}. Observations of X-rays with the *EXOSAT* satellite from three novae indicate that the WD remained luminous—after contracting at the end of the mass-loss phase—for at least one year for Nova PW Vul 1984 and Nova Vul 1984 No. 2, and for almost 3 years for Nova GQ Mus 1983. An even longer constant luminosity phase (~ 5.5 yr $\approx 50t_3$) is inferred for GQ Mus from a later study of the optical emission-line spectrum (Krautter & Williams 1989). The value of t_3 may therefore be roughly approximated by either t_{m-1} or $\sim 0.1t_{3bol}$.

The maximal versus average velocities are plotted in Figure 8. The difference between them increases with increasing v_{av}. Thus, the higher the velocities obtained, the wider is the *range* of velocities for a given object. Phases of relatively low expansion velocities are always encountered.

A well-known characteristic of nova outbursts is that only a small amount of hydrogen needs to be burnt in order to supply the energy required for expansion, mass ejection at high velocities, and radiation. Most of the energy produced is spent in overcoming the high gravitational potential of the WD. The high helium content observed in nova ejecta has a different source: at the end of an outburst, when mass loss ceases, a remnant hydrogen-rich shell is left on the WD and the hydrogen in this shell is burnt into helium before and during the decline of the nova (bolometric) luminosity. At the onset of the next outburst, a convective envelope forms, in which this remnant shell becomes mixed with the accreted material and with an underlying layer of the WD core, thus providing a larger helium/hydrogen ratio than in the accreted material, in agreement with observations. As it turns out, for massive WDs, the energy required for expansion entails burning—during outburst—of a larger, non-negligible, fraction of the accreted

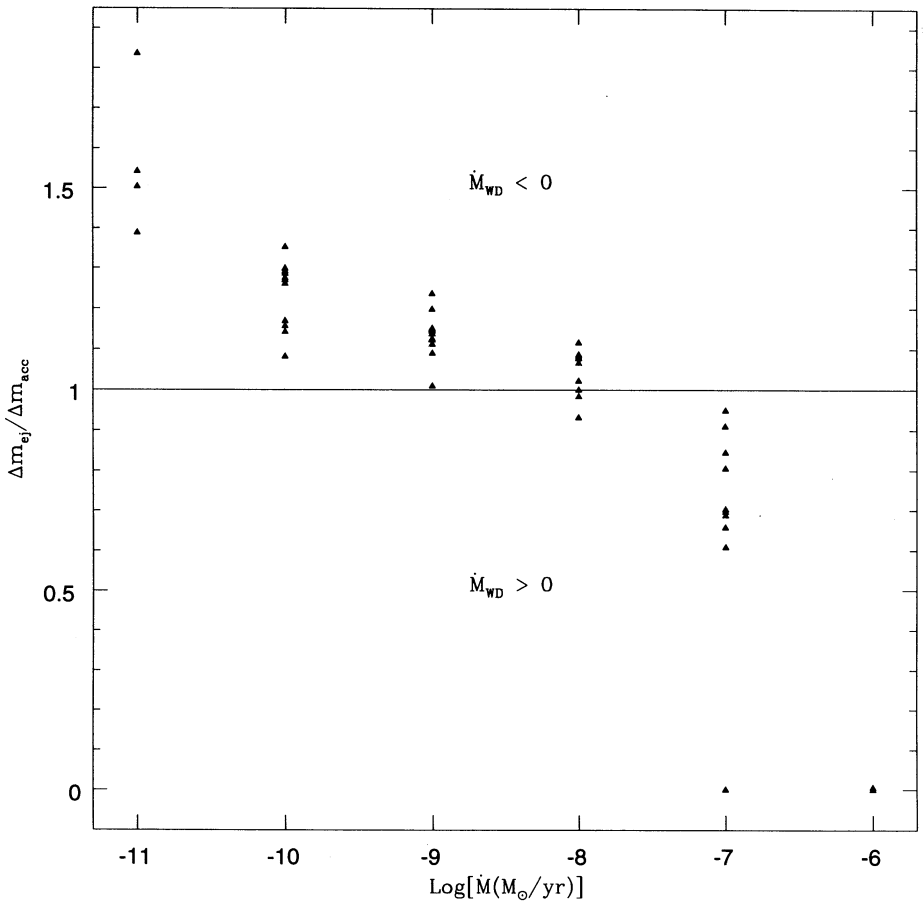

FIG. 6.—Ratio of ejected to accreted mass as a function of accretion rate (on a logarithmic scale). The horizontal line corresponds to M_{WD} = constant; the WD mass increases secularly below this line and decreases above it.

hydrogen, which constitutes an additional source of helium for the ejecta (Kovetz & Prialnik 1994). The amount of hydrogen burnt during outburst, as a function of M_{WD}, is shown in Figure 9 for all models. In conclusion, while relatively high helium abundances may be obtained over the entire M_{WD} range, a helium/hydrogen mass ratio in excess of 1 in the ejecta should indicate a massive WD. The highest He/H obtained is $\sim$4. This is also the highest value ever obtained from observations: it occurred in the ejecta of RN U Sco (Williams et al. 1981).

4. NOVA THEORY VERSUS OBSERVATIONS

4.1. *Types of Outburst*

In the last column of Table 2 we have identified our models with different types of nova outbursts. The criteria adopted for distinguishing between classes are based on typical characteristics of observed systems. Often, however, the classification is ambiguous.

1. If 10 yr $\leq P_{rec} \leq$ 100 yr and mass is ejected, the model is considered a RN.

2. If $t_{3bol} \geq 10$ yr and the amplitude of the outburst is moderate, $4 < A < 10$, the model represents a symbiotic nova (SymN). Mass ejection with very low expansion velocities is detected in some SymN (Kenyon 1986); others do not show evidence for mass loss (Munari 1992; Munari et al. 1992). Among our SymN models, we also obtain ejecting and non-ejecting types. If mass loss occurs, we require $t_{m-1} \geq 1$ yr for SymN.

3. The distinction between a symbiotic nova model and a very slow classical nova model is made according to the amplitude of the outburst. Thus, if $A > 10$, mass loss occurs and $t_{m-1} \geq 1$ yr, the model is considered a very slow classical nova (NVS).

4. Generally, the distinction between different classical nova speed classes is somewhat arbitrary, since they do not represent different types of phenomena. Nova properties, in particular t_3, vary continuously between the highest and the lowest observed values. The same applies to the calculated decline times t_{3bol} and the duration of mass loss episodes t_{m-1}. As the latter is closer to the observed t_3, we base the classification criterion on its value: if 100 days $\leq t_{m-1} <$ 1 yr, the model is considered a slow nova (NS); if 50 days $\leq t_{m-1} <$ 100 days, it is considered a moderately fast nova (NM); if 10 days $\leq t_{m-1} <$ 50 days, a fast nova (NF); and if $t_{m-1} <$ 10 days, a very fast nova (NVF).

In conclusion, accretion onto low-mass WDs leads to outbursts typical of symbiotic and very slow novae. We note that, observationally, there are systems which have been classified as both, e.g., RR Tel or V407 Cyg (Allen 1980; Kenyon 1986). The common feature of these systems is, therefore, the WD's mass. Moving to higher WD masses, we encounter faster outbursts—slow, moderate and fast novae—and at still higher masses, very

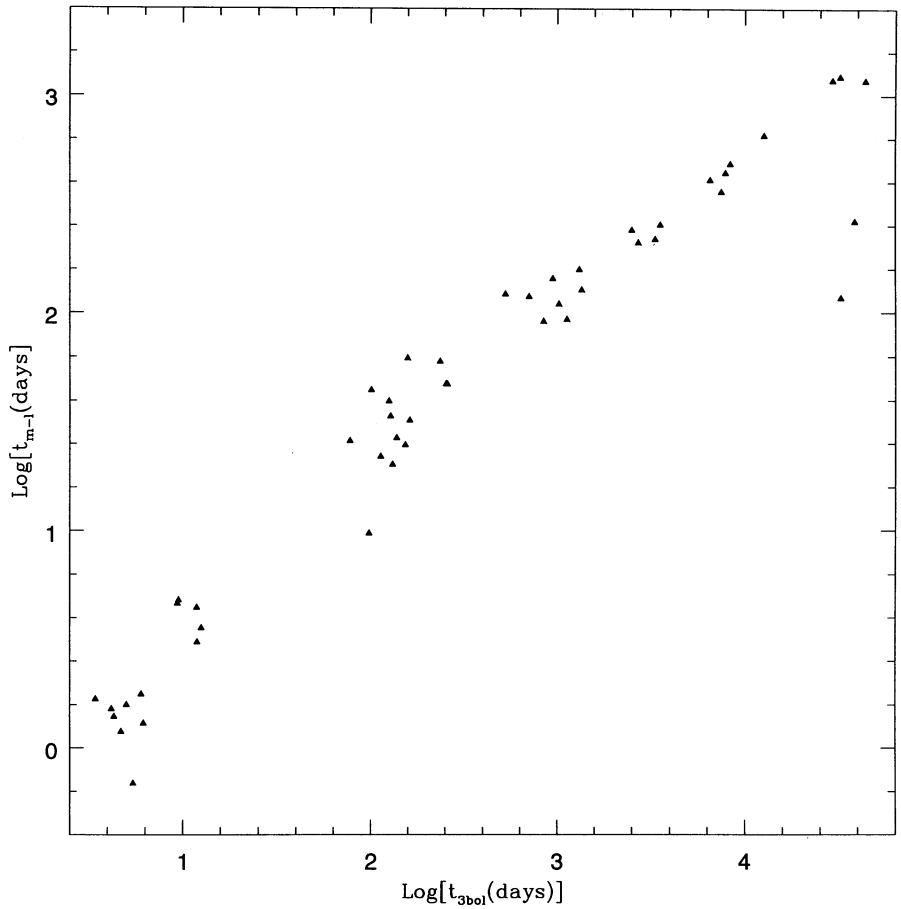

FIG. 7.—Duration of the mass loss phase vs. time of decline of the bolometric luminosity by 3 mag, on logarithmic scales

fast novae appear. For the highest WD mass, near the Chandrasekhar limit, *only* very fast novae are obtained. The only models which appear to have no observational counterparts are those corresponding to the highest accretion rate, in all M_{WD} and T_{WD} ranges. These models, however, tend to a steady state, with continuous burning (see Kovetz & Prialnik 1994) and as such they should be indistinguishable from AGB stars in late stages of evolution. Eventually, when a sufficiently massive helium layer builds up, a helium shell flash may occur, which might closely resemble a nova outburst. Such events are, however, beyond the scope of this paper. Another problem is posed by models of 1.4 $M_\odot$ with accretion rates of 10^{-7} $M_\odot$ yr^{-1}. These are characterized by frequent eruptions (at intervals of $\sim$8 months), short decline times ($t_{3bol} \approx 10$ days and $t_{m-1} \approx 4$ days) and amplitudes of $\sim$6 mag. Ejected masses are $\sim 8 \times 10^{-8}$ $M_\odot$, with velocities of the order of 1000 km s^{-1}. Since this behavior is typical of very massive WDs, increasing in mass on their short way to collapse, it should be very difficult to detect. If detected, however, it might indicate an impending collapse.

The parameter space where RN can occur is shown in Figure 10; it is limited by the constraints: 10 yr $\geq P_{rec} \geq$ 100 yr and $m_{ej} > 5 \times 10^{-8}$. Of our present 64 models, nine are found in this range. The recurrence time of nova outbursts is inversely proportional to $\dot{M}$, as well as to some power of M_{WD}. This is the reason for assuming that recurrent novae must be obtained by accretion at a high rate onto massive WDs (Starrfield et al. 1985; Starrfield et al. 1988; Truran et al. 1988; Kato 1990, 1991; Kovetz & Prialnik 1994). It turns out, however, that while RN *do* require $\dot{M} \geq 10^{-8}$ $M_\odot$ yr^{-1}, the constraint on M_{WD} is less severe. Short recurrence times may be obtained for M_{WD} down to ~ 1 $M_\odot$. We thus find that decline times do not need to be very short, as would be the case if RN precursors were only very massive WDs. We note that the decline times of RN span the entire CN range, from 280 days for V616 Mon, to 113 days for T Pyx and down to 6 days for U Sco. Different velocities may be obtained and ejected shells may be as massive as 10^{-5} $M_\odot$. Only if a RN is very fast and ejects a small amount of material at very high velocities, would it follow that the erupting WD is extremely massive. If, in addition, the ejecta has a relatively high Z, it would mean that the WD is also cold.

4.2. *Correlations between Outburst Properties*

The most striking feature that emerges from the observation of novae is the correlation between t_3 (or t_2) and M_B. This correlation seems to be so well established that novae are used as standard candles for distance determinations (e.g., Cohen 1985). Nevertheless, the correlation is not tight and is represented by a wide strip, rather than a line. Two questions arise: (a) Do the calculations reproduce the observed correlation? (b) Could the correlation be improved by better observational data, or is the spread intrinsic? The results of our calculations (for both t_{m-1} and t_{3bol}) are shown in Figure 11,

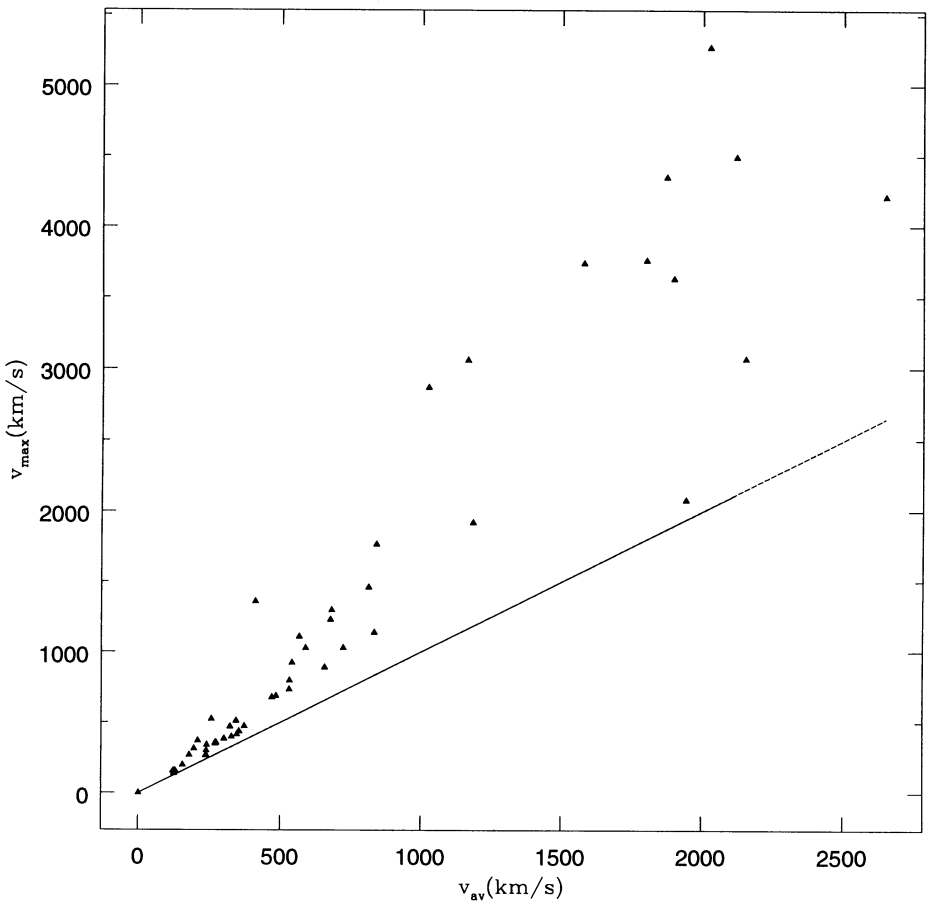

FIG. 8.—Maximal velocities of the ejecta vs. mass-averaged velocities. The solid line corresponds to constant (maximal = average) ejection velocities. Deviations from this line are proportional to the spread of velocities for a given nova outburst.

together with the linear fit of Pfau (1976) to the observational data. A larger sample of novae yields a very similar band (Shara 1981), emphasizing at the same time the large spread of points. Firstly we note that the entire observed range is covered by the models—a fact which is, in itself, encouraging. Secondly, the slope of the calculated points is less steep than the observational one, especially toward short decline times. The discrepancy may be due to two factors: at short decline times t_{m-1} becomes a poor approximation to t_3 (and the longer t_{3bol} might provide a better approximation), and, perhaps more importantly, the calculated L_{max}, as given in Table 2, may be in error (underestimated), as mentioned in § 3. Both factors should lead to a closer agreement between theory and observations. Regardless of this discrepancy, however, it is quite obvious that the spread of points occurs naturally, as the result of the effect of T_{WD} and $\dot{M}$ on both L_{max} and t_3, in addition to the more dominant effect of M_{WD}. Thus novae should not be expected to improve as distance indicators. We note that there is also an obvious correlation between L_{max} and the time of decline of the bolometric luminosity. The slope of this relation is significantly shallower than the slope of (L_{max}, t_{m-1}).

A less marked, but still obvious correlation may be shown to exist between t_3 and the average expansion velocities deduced from nova spectra (McLaughlin 1960), although systems of very different velocities are often observed in the same nova shell. The results obtained here for v_{av} are shown in Figure 12. A sample of 12 well-observed novae (T Aur 1891, RR Pic 1925, DQ Her 1934, CP Lac 1936, HR Del 1967, V1500 Cyg 1975, V1668 Cyg, 1978, V693 CrA 1981, GQ Mus 1983, PW Vul 1984, QU Vul 1984, QV Vul 1987), for which composition, average expansion velocities, and ejected masses are determined will be used for comparison. The sample does not include nova Aql 1370, which has an extremely unusual and uncertain composition (Snijders et al. 1987). The corresponding points are also plotted in Figure 12. We find an excellent agreement between theory and observations, bearing in mind the uncertainties in both. We note that the clustering of computational points may be misleading. It has nothing to do with the frequency of occurrence of corresponding objects; it only means that many parameter combinations (which may rarely occur in reality) lead to similar results. By the same token, a cluster of observational points needs only a single nearby calculated point (parameter combination) to account for them.

4.3. *Uncorrelated Characteristics*

One of the puzzling traits of CNs is the lack of correlation between t_3 and Z_{ej}, which appears to contradict the straightforward theory: a strong outburst is obtained when the envelope has a high CNO mass fraction and such an outburst should lead to a rapid development, i.e., a rapid decline. The intricate interplay of the three basic parameters in this theory is illustrated by the same lack of correlation that results from

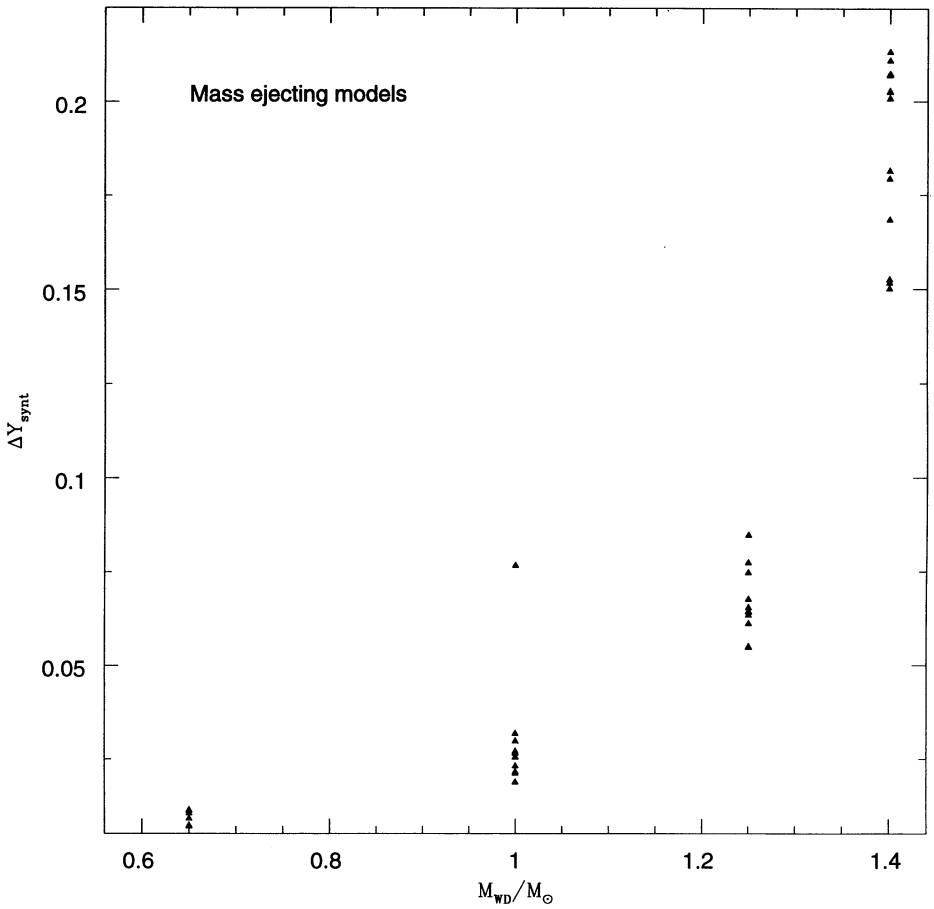

FIG. 9.—Amount of helium (in terms of mass fractions) synthesized at the peak of a nova outburst (prior to and during the mass-loss phase) as a function of the WD mass.

model calculations, as shown in Figure 13. Thus, enhanced CNO is a sufficient, but not a necessary condition for strong outbursts, and strong outbursts are not necessarily short-lived, for example, in cases where the ejection of large shells ensues. The agreement (overlap) between theory and observations is quite remarkable. Incidentally, a slow nova with a high Z ejecta—like DQ Her 1934—may be obtained for a 1 $M_\odot$ hot WD, accreting at an average rate of 10^{-11}–10^{-10} $M_\odot$ yr^{-1}, as seen in Tables 1 and 2. Such a nova should have moderate to low expansion velocities (like DQ Her) and an ejected shell mass of the order of 10^{-5} $M_\odot$ (smaller than that estimated for DQ Her).

A third independent characteristic of nova outbursts appears to be Y_{ej}. It is not correlated to either t_3 or Z_{ej}, and this behavior persists if only a subsample of the observational data is considered, for which one of these parameters is more or less constant (Prialnik 1995). Again, this trait is verified by the models, as shown in Figure 14, where Z_{ej} versus Y_{ej} is

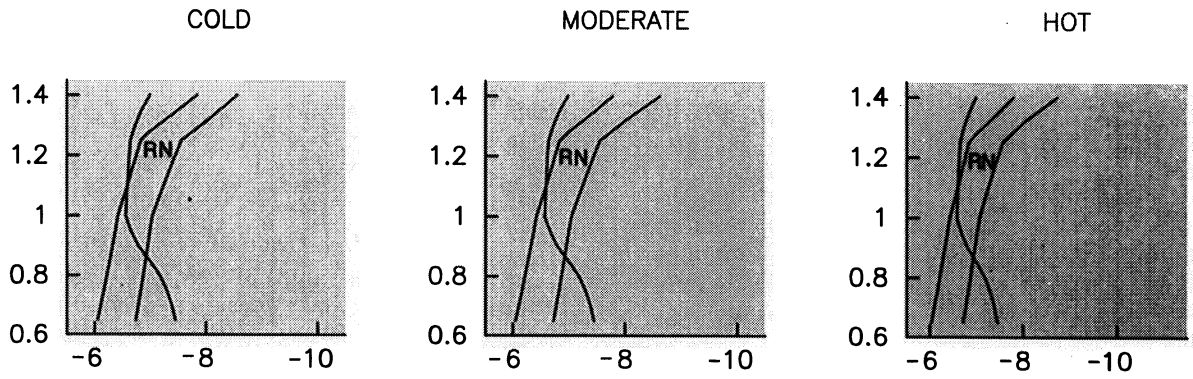

FIG. 10.—Region of recurrent novae—defined by the requirements 10 yr < P_{rec} < 100 yr and $m_{ej} > 5 \times 10^{-8}$ $M_\odot$—in the ($\dot{M}$, M_{WD}) plane for each of the three WD temperatures (see Fig. 3), between contours of constant recurrence periods of 10 yr and 100 yr and above (to the right) the line corresponding to $m_{ej} = 5 \times 10^{-8} M_\odot$.

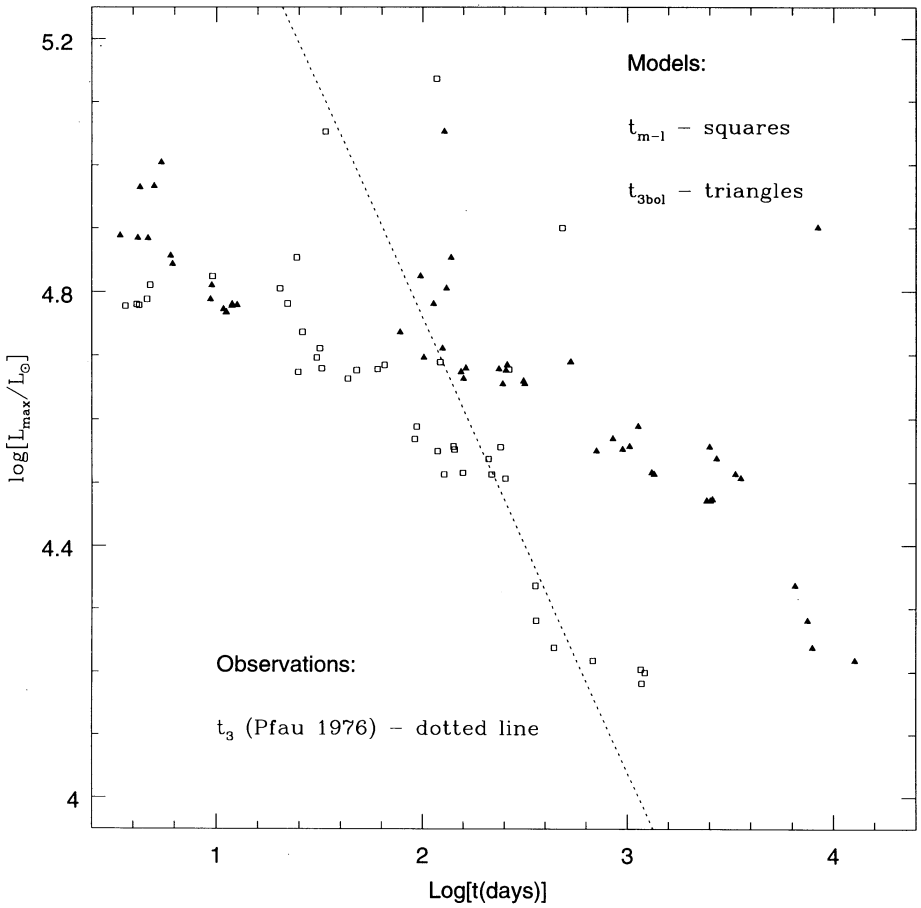

FIG. 11.—Maximum (bolometric) luminosity obtained at outburst (see text) vs. time of decline; open squares correspond to the mass loss time t_{m-1}, a close lower limit to the visual t_3, and filled triangles correspond to the time of decline of the bolometric luminosity by 3 magnitudes. The dotted line represents Pfau's (1976) fit derived from observations.

plotted for models and for the observed novae. It should, perhaps, be mentioned that, according to the nova theory, Z_{ej} is determined by pre-outburst evolution (the outcome of diffusion and convection); t_3 is characteristic of the outburst itself (the expansion and consequent mass loss); and Y_{ej} is the result of post-outburst evolution (burning of the remnant left over after mass loss). It is, therefore, to be expected that these characteristics should be independent of each other.

We end this section on a speculative note. The two characteristics of novae that can be straightforwardly determined by observations are the time of decline, e.g., t_3, and the amplitude of the nova outburst A (the difference between minimum and maximum magnitudes, which is independent of distance). The data provided by Duerbeck's (1987) catalog was analyzed by Vogt (1990), who found a correlation between A and t_3, with a slope similar (within errors) to that of the (M_B, t_3) correlation. This implies a restricted range of absolute minimum magnitudes (and hence accretion rates) during times of the order of decades prior to or following an outburst—the times of observation of the low-state magnitude. This is in agreement with Patterson's (1984) results and conclusions regarding the high $\dot{M}$ of CNs near outburst, based on novae with known distances, and with the results obtained by Warner (1987). In Figure 15 we plot the results obtained in the present calculations in the (A, t_{m-1}) plane. There is no apparent correlation, although statistical factors (leading to selection effects) have not been considered in the case of the models. Moreover, in order to reproduce the entire range of observed nova characteristics, a wide range of accretion rates is required for the models, implying a wide range of minimum luminosities. This apparent discrepancy with observations provides indirect support to the "hibernation hypothesis" (Shara et al. 1986; Prialnik & Shara 1986): the mass transfer rate decreases several decades after outburst by a factor of 10 to 100, remains low for a long period of time and then increases again, thus inducing a new outburst. Therefore, the mean accretion rate, which prevails for most of the time between CN outbursts, is different (lower) than that observed for most known novae. Observational support for hibernation, based on observations at different times after decline has been provided by Warner (1987), Vogt (1990), and Duerbeck (1992). The constant mass accretion rates adopted in our calculations represent these *mean* accretion rates. In conclusion, our calculations predict (deep) quiescence luminosities—mainly determined by $\dot{M}$—that vary considerably from system to system. Since they are uncorrelated with t_3, the resulting amplitude (the ratio of maximal to minimal luminosity) becomes independent of t_3, in spite of the dependence of the maximal luminosity on t_3. Our calculations also imply a weak (or no) dependence of the hibernation mass transfer rate on the mass transfer rate close to

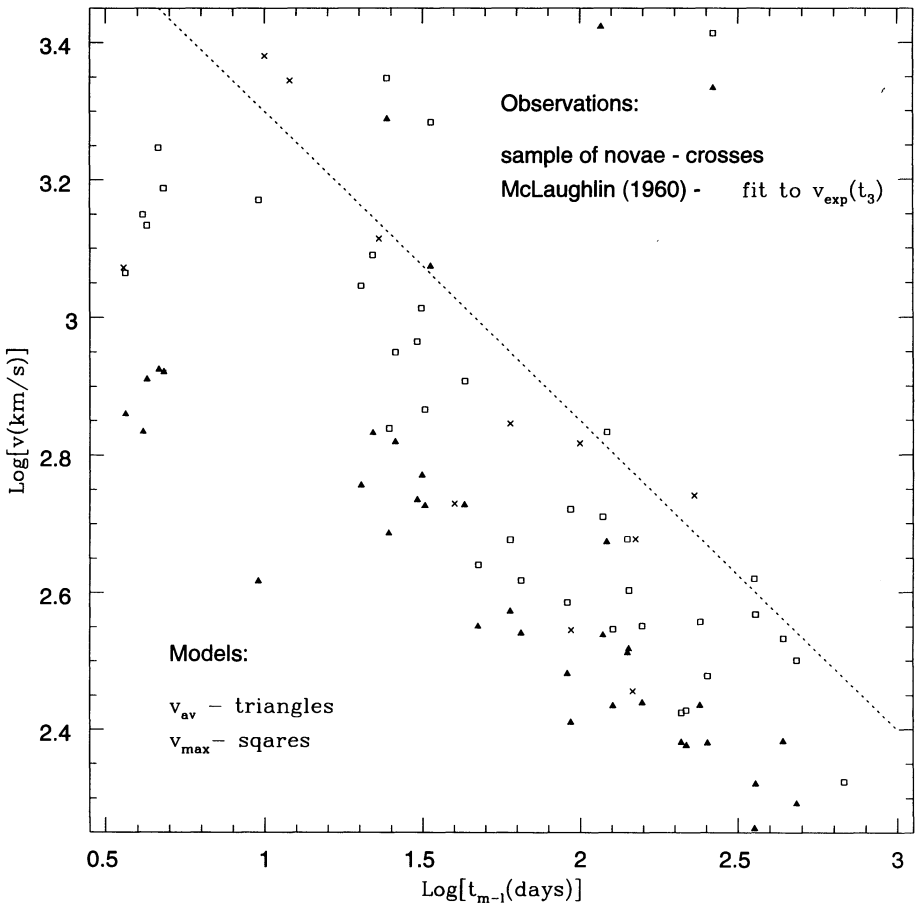

FIG. 12.—Expansion velocity vs. mass-loss time (or t_3) on logarithmic scales: filled triangles correspond to average velocities; open squares correspond to maximal velocities; crosses correspond to observed novae. The dotted line represents a linear fit (McLaughlin 1960) derived from early observations of expansion velocities and visual decline times.

outburst, meaning that mass transfer during these different phases may be triggered by different mechanisms.

4.4. *Derivation of Unknown Properties*

We have seen that among the observed nova characteristics, three are independent: t_3, Y_{ej}, and Z_{ej}. Our evolutionary sequences yield the values of the functions t_{3bol} (M_{WD}, T_{WD}, $\dot{M}$), Y_{ej} (M_{WD}, T_{WD}, $\dot{M}$) and Z_{ej} (M_{WD}, T_{WD}, $\dot{M}$) over the parameter grid. For a well-observed nova, with determined t_3, Y_{ej}, and Z_{ej}, we can obtain M_{WD} (t_3, Y_{ej}, Z_{ej}), T_{WD} (t_3, Y_{ej}, Z_{ej}) and $\dot{M}(t_3, Y_{ej}, Z_{ej})$ by inverting these relations. If a solution exists and if it is unique, we can obtain the mass of the nova progenitor, its temperature, and an estimate for the average mass transfer rate. In the few cases in which the white dwarf mass has been determined by observations, the inverse relation $M_{WD}(t_3, Y_{ej}, Z_{ej})$ can of course be directly tested. We may also derive other observable properties, such as the expansion velocity or the ejected mass, and compare them with those actually observed. Unfortunately, this procedure may be as yet premature. From the observational point of view, abundance determinations for nova shells are extremely uncertain (Livio & Truran 1994). From the theoretical point of view, the exact decline time in the visual, or in the blue, is difficult to determine, because in a calculation of a nova outburst, the ejected material, which forms an opaque shell, is not included. We could adopt observed expansion velocities instead of t_3, since they are closely correlated, but these are as ambiguous as the abundances. Moreover, in reality and in the model calculation, many different velocities are obtained for a given object (at different times, or at different spectral phases). But, in principle, this method *is valid*, even if, for the time being, it should be applied and regarded with some caution. Since it is based on the simultaneous match of *three* parameters (and, for a given WD composition, there can be only three in a semi-detached binary system, when age is also a factor) it is a far more accurate method than those based on a single parameter match. As an example, we choose Nova PW Vul 1984 with $t_3 = 147$ days, $Y_{ej} = 0.28$ and $Z_{ej} = 0.18$. Our interpolation procedure is based on properties which are defined over the entire grid. We thus use t_{3bol} rather than t_{m-1}. Assuming $t_{3bol} \approx 10t_3 \approx 1500$ day (see § 3.3), we draw contours corresponding to these values in the ($\dot{M}$, M_{WD}) plane for each of the three temperatures. The results are shown in Figure 16. The three lines intersect for the moderate temperature, at a point corresponding to $M_{WD} \sim 0.9\ M_\odot$ and $\dot{M} \sim 5 \times 10^{-10}\ M_\odot\ \mathrm{yr}^{-1}$. Other properties may now be obtained by interpolating between our models. We find $v_{av} \approx 290\ \mathrm{km\ s}^{-1}$, as compared to the observed 285 km s^{-1}, and $m_{ej} \approx 4 \times 10^{-5}\ M_\odot$, significantly lower than the observationally derived value ($\sim 30 \times 10^{-5}\ M_\odot$). In fact, by this procedure, we systematically obtain a fair agreement with

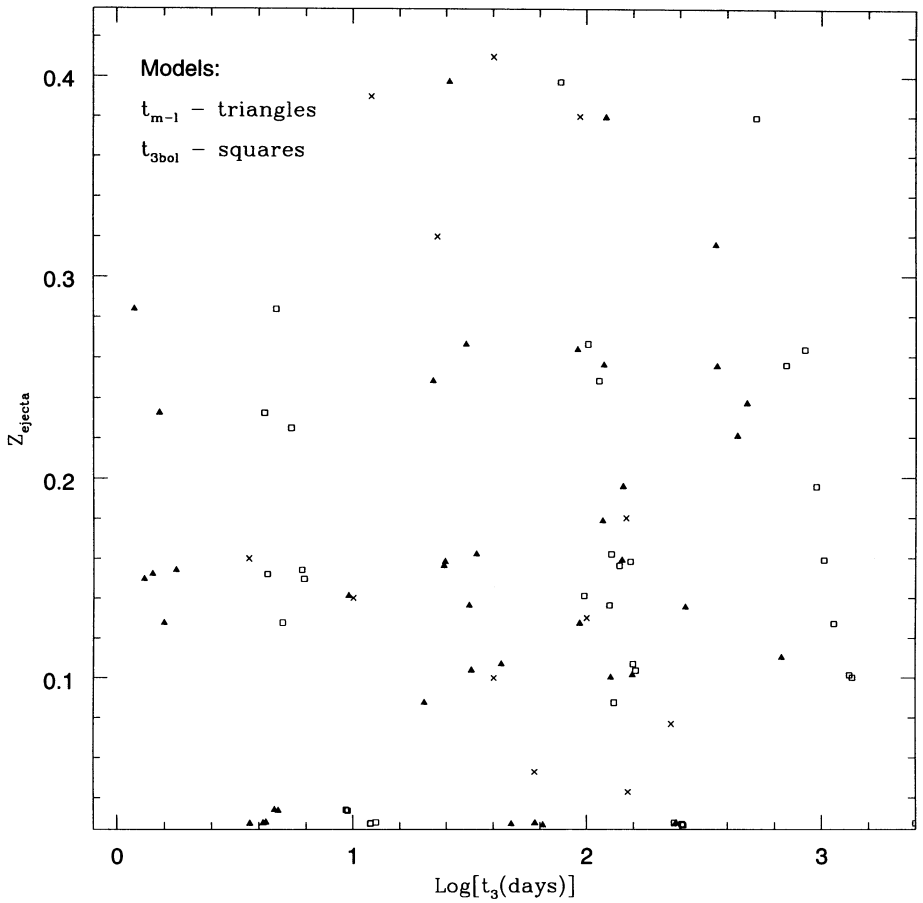

FIG. 13.—Heavy element content of the ejecta Z_{ej} vs. time of decline by 3 magnitudes for a sample of well-observed novae (*crosses*). The model results are indicated by filled triangles, corresponding to the mass loss time (a close lower limit to t_3), and by open squares, corresponding to the decline time of the bolometric luminosity by 3 magnitudes. The lack of correlation in all three cases is apparent.

observations for expansion velocities, but lower than observed ejected masses. There is, however, a large uncertainty in the observational estimates of nova shell masses, especially in view of the clumpiness of these shells (Barger et al. 1993; Saizar & Ferland 1994), which is best shown by recent *HST* observations. These estimates rely on filling factors that are very difficult to guess.

5. CONCLUSIONS

We have performed a systematic study of the evolution of accreting WDs through several cycles, covering what we regard as the major part of the three-dimensional (M_{WD}, T_{WD}, $\dot{M}$) parameter space. We have considered homogeneous CO WDs and mixing between the accreted matter and the underlying WD core was assumed to take place via the diffusion-convection mechanism. We did not address in this paper the detailed composition of the ejecta, but only the mass fractions Y_{ej} and Z_{ej} (of course, $X_{ej} = 1 - Y_{ej} - Z_{ej}$). It is believed that very massive WDs ($M_{WD} > 1.35\ M_\odot$) may be composed of ONeMg rather than CO. The WD structure would not be affected by this change, but diffusion could be. Nevertheless, the results should not differ considerably from those obtained with a CO WD (see Prialnik & Shara 1995), except, of course, for the break-up of heavy elements.

The main results of this study may be summarized as follows:

1. The TNR-triggered outburst mechanism can explain many different types of novae: CNs of all speed classes, including extremely rapid and extremely slow ones, SymNs and RNs.

2. The entire range of observed nova characteristics (with very few exceptions, such as $Z = 0.86$ or $A = 19$ magnitudes) is covered by the grid of models. Unusual combinations of properties, such as a high Z slow nova, *can* be obtained for suitable parameter combinations. We note, in particular, that CNs can be obtained adopting accretion rates as high as 10^{-8} $M_\odot$ yr^{-1}, but the range of properties reproduced with such rates is restricted. If a better understanding of the observations should confine the ranges of properties typical of CNs (such as Z, m_{ej}, v), then it might be possible to explain novae within a narrow range of high accretion rates. But the observational evidence available so far seems to point to the opposite.

3. We determine the region of parameter space that leads to recurrent novae: we find that the precursors of such novae can be nonmassive WDs ($M_{WD} \geq 1\ M_\odot$). Thus RNs can occur within any CN speed class: from slow ($t_3 \sim 100$ days) to very fast ($t_3 < 10$ days), in agreement with observations.

4. The mass of the accreting WD increases if $\dot{M} \geq 10^{-7}\ M_\odot$ yr^{-1} and decreases if $\dot{M} \leq 10^{-9}\ M_\odot$ yr^{-1}, independently of the WD's mass and temperature. In the narrow intermediate

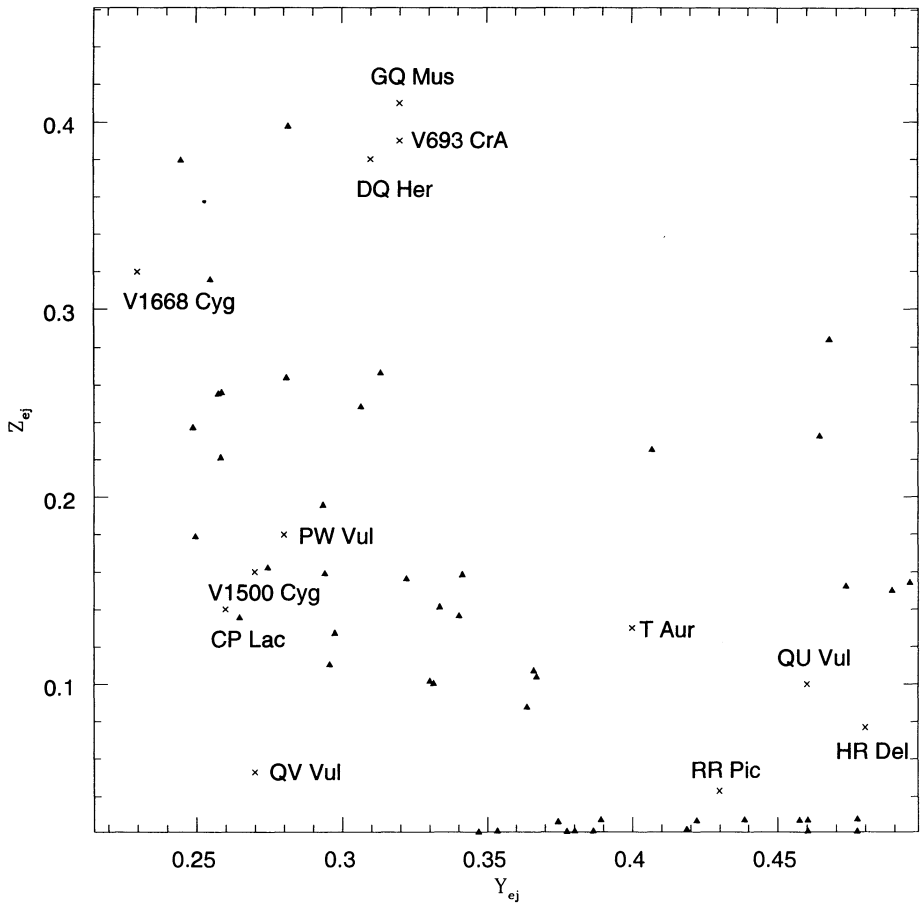

FIG. 14.—Heavy element mass fraction of the ejecta Z_{ej} vs. the corresponding helium mass fraction Y_{ej} for observed novae (*crosses*) and for models (*triangles*)

range of accretion rates the WD's fate depends mainly on its temperature: cold WDs lose mass, whereas hot ones gain mass, while their mass is relatively low. For a hot WD, if the accretion rate remains constant, the WD's mass will grow only up to the point where the sign of $\dot{M}_{WD}$ is reversed. The conclusion is that the Chandrasekhar limit may be reached only at accretion rates in excess of $10^{-8}\ M_{\odot}\ \mathrm{yr}^{-1}$. This is also the range of accretion rates that leads to symbiotic novae, which may thus be considered as possible precursors of Type Ia supernovae, as suggested by Iben & Tutukov (1984) and, more recently, by Munari & Renzini (1992).

5. We find that for most parameter combinations, the computed masses of the ejecta are lower than those derived from observations, although the entire observed range is reproduced. We should point out that the effect of the secondary star moving within the nova envelope might enhance mass ejection (Livio et al. 1990). This effect, however, is not significant, since the ejected material can amount to—at most—the entire mass of the envelope (lying above the burning shell). The ejected mass obtained in our calculations is already a very large fraction of the envelope mass, so that the difference between them would be insignificant. It is only significant in the determination of m_{ej} relative to m_{acc}, concerning the sign of $\dot{M}_{WD}$.

6. The maximum luminosities obtained are still somewhat problematic when compared to observations, particularly of very fast novae. These luminosities are well above the Eddington luminosities (calculated assuming electron scattering opacities), but not as high as those sometimes inferred from observations, which can surpass the Eddington limit by factors of 10 or more.

7. The calculated velocities are in very good agreement with the observations. We distinguish between the mass averaged velocity and the maximal velocity obtained for each model. We find that the range of velocities obtained for a given object is wider for higher maximal velocities.

8. We find a distinct correlation between the duration of the mass loss phase and the time of decline of the bolometric luminosity (which may be much longer than the observed time of decline in the visual): t_{3bol} is roughly an order of magnitude higher than t_{m-1}.

9. Correlations are obtained between the peak luminosity and time of decline, as well as velocity and time of decline, compatible with those derived from observations. It is shown that these correlations cannot be tight, as would be the case if novae were a one parameter family of events. The WD's mass is in this case the key parameter, the sensitivity of the evolution pattern to the other two parameters causing significant deviations from a well distinguishable mean. The implication is that novae cannot be considered accurate distance indicators. Deviations from the mean are not spurious; they are intrinsic.

10. Three nova properties are shown to be independent (uncorrelated): the helium and the heavy element content of the ejecta and the time of decline. This conclusion, based on observations (see Prialnik 1995), is supported by our calcu-

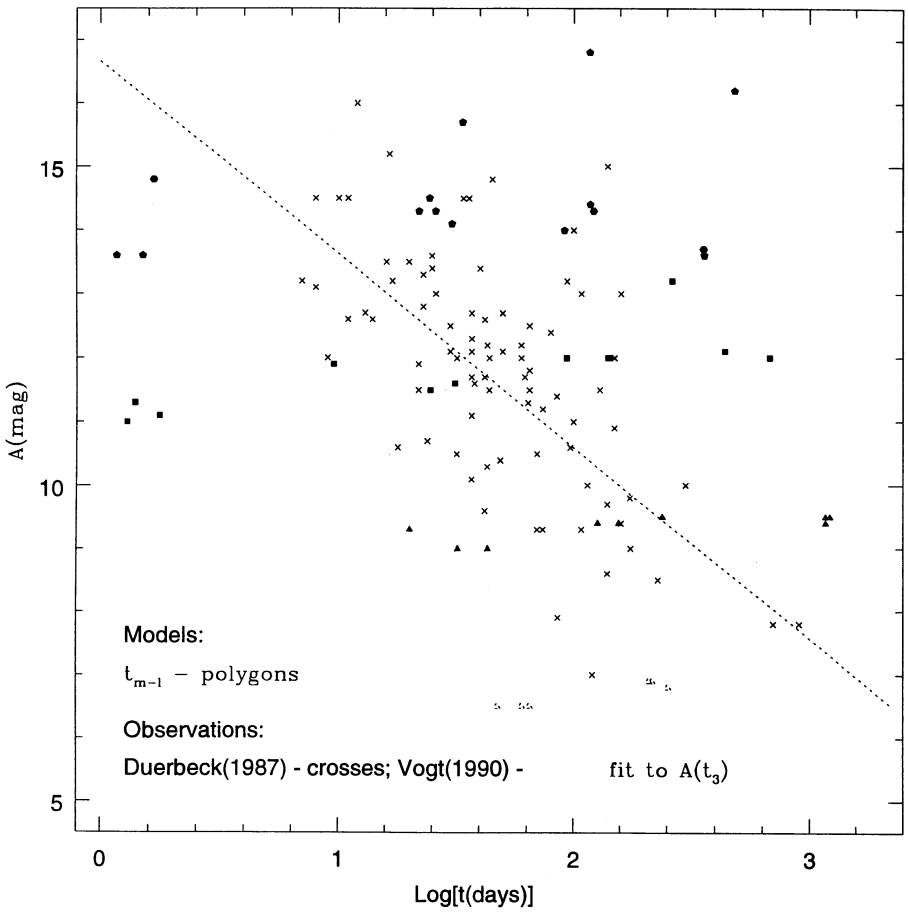

FIG. 15.—Outburst amplitude (see text) A vs. time of decline. Crosses represent observations (Duerbeck 1987) and the dotted line is Vogt's (1990) linear fit to the observed values. Polygons represent model results, grouped according to the accretion rate: (*triangles*) $10^{-8}\ M_\odot\ \mathrm{yr}^{-1}$; (*squares*) $10^{-9}\ M_\odot\ \mathrm{yr}^{-1}$; (*pentagons*) $10^{-10}\ M_\odot\ \mathrm{yr}^{-1}$; (*hexagons*) $10^{-11}\ M_\odot\ \mathrm{yr}^{-1}$.

lations. In principle, a transformation is possible from the three basic independent parameters to the three observable uncorrelated properties: M_{WD} (t_3, Y_{ej}, Z_{ej}), $\dot{M}$ (t_3, Y_{ej}, Z_{ej}), and T_{WD} (t_3, Y_{ej}, Z_{ej}). Such a transformation should provide the mass, the temperature, and the average rate of accretion of a nova progenitor, provided the composition of the nova shell is well determined from observations, and the time of decline is accurately estimated by the theory. We can then test the agreement between theory and observations regarding other characteristics—such as the expansion velocity and the ejected mass (see 5 and 7 above).

The theory of nova outbursts seems to have gone a long way since the early calculations of about two decades ago, but we are not yet at the end of the road and, more than ever, we depend on the accurate results of observations to guide us further.

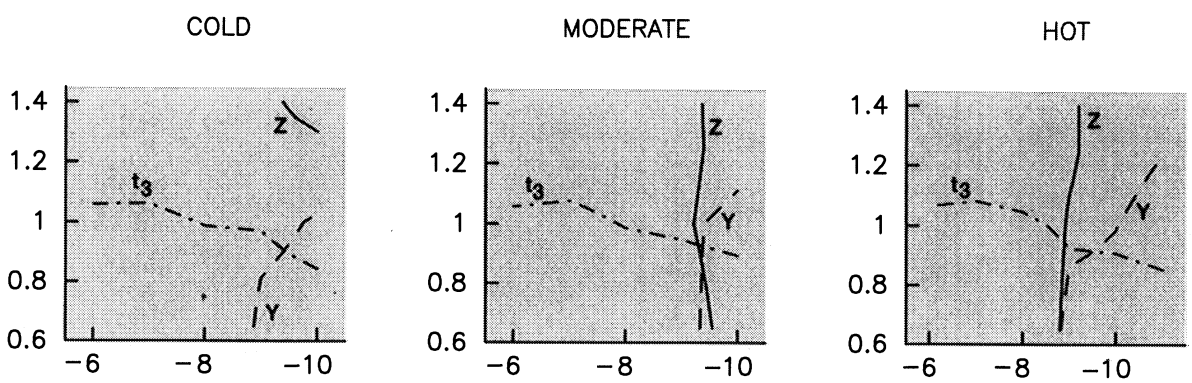

FIG. 16.—Example of the derivation of nova parameter from observations, for Nova PW Vul 84. The solid line is the $Z = 0.18$ contour in parameter space (for each of the three WD temperatures); the dashed line is the $Y_{\mathrm{ej}} = 0.28$ contour and the dash-dotted line is the $t_{3\mathrm{bol}} = 1500$ days contour. An intersection is obtained in the middle panel, indicating a WD mass of 0.9 $M_\odot$ and an accretion rate of $\sim 5 \times 10^{-10}\ M_\odot\ \mathrm{yr}^{-1}$.

We are grateful to Mike Shara, Bob Williams, Hilmar Duerbeck, and Brian Warner for useful discussions. We acknowledge support by the Director's Discretionary Research Fund at the Space Telescope Science Institute. This research was supported in part by the Israel Science Foundation administered by the Israel Academy of Sciences and Humanities.

REFERENCES

Allen, D. A. 1980, MNRAS, 192, 521
Barger, A. J., Gallagher, J. S., Bjorkman, K. S., Johansen, K. A., & Nordsieck, K. H. 1993, ApJ, 419, L85
Cassatella, A., & Viotti, R., eds. 1990, Physics of Classical Novae (Berlin: Springer)
Cassinelli, J. P., & Castor, J. I. 1973, ApJ, 179, 189
Caughlan, G. R., & Fowler, W. A. 1988, Atomic Data Nucl. Data Tables, 40, 283
Cohen, J. G. 1985, ApJ, 292, 90
Della Valle, M., & Livio, M. 1994, ApJ, 423, L31
Duerbeck, H. W. 1987, Space Sci. Rev., 45, 1
———. 1992, MNRAS, 258, 629
Fujimoto, M. Y. 1982a, ApJ, 257, 752
———. 1982b, ApJ, 257, 767
Iben, I., Jr., Fujimoto, M. Y., & MacDonald, J. 1992, ApJ, 388, 521
Iben, I., Jr., & Tutukov, A. V. 1984, ApJS, 54, 335
Kato, M. 1990, ApJ, 355, 277
———. 1991, ApJ, 366, 471
Kato, M., & Iben, I., Jr. 1992, ApJ, 394, L47
Kenyon, S. J. 1986, The Symbiotic Stars (Cambridge: Cambridge Univ. Press)
Kovetz, A., & Prialnik, D. 1985, ApJ, 291, 812
———. 1994, ApJ, 424, 319
Kovetz, A., & Shaviv, G. 1994, ApJ, 426, 787
Krautter, J., & Williams, R. E. 1989, ApJ, 341, 968
Lance, C. M., McCall, M. L., & Uomoto, A. K. 1988, ApJS, 66, 151
Livio, M. 1992, ApJ, 393, 516
———. 1994, in Interacting Binaries, ed. H. Nussbaumer & A. Orr (Berlin: Springer), 135
———. 1993, in Cataclysmic Variables and Related Physics, ed. O. Regev & G. Shaviv (Bristol: Institute of Physics Publishing), 57
——. 1995, in ASP Conf. Ser. Millisecond Pulsars: A Decade of Surprise, ed. A. Fruchter, M. Tavani, & D. Backer (San Francisco: ASP), in press
Livio, M., Shankar, A., Burkert, A., & Truran, J. W. 1990, ApJ, 356, 250
Livio, M., & Truran, J. W. 1994, ApJ, 425, 797
MacDonald, J. 1983, ApJ, 267, 732
McLaughlin, D. B. 1960, in Stellar Atmospheres, ed. J. L. Greenstein (Chicago: Univ. Chicago Press), 585
Mihalas, D. 1978, Stellar Atmospheres 2d ed. (San Francisco: Freeman)
Munari, U. 1992, A&A, 257, 163
Munari, U., & Renzini, A. 1992, ApJ, 397, L87
Munari, U., Whitelock, P. A., Gilmore, A. C., Blanco, C., Massone, G., & Schmeer, P. 1992, AJ, 104, 262
Ögelman, H., Krautter, J., & Beuermann, K. 1987, A&A, 177, 110
Patterson, J. 1984, ApJS, 54, 443
Payne-Gaposhkin, C. 1957, The Galactic Novae (Amsterdam: North Holland)
Pfau, W. 1976, A&A, 50, 113
Prialnik, D. 1993, in Cataclysmic Variables and Related Physics, ed. O. Regev & G. Shaviv (Bristol: Institute of Physics Publishing), 351
———. 1986, ApJ, 310, 222
———. 1995, in Cataclysmic Variables and Related Objects, ed. A. Bianchini & M. Orio (Bristol: Institute of Physics Publishing), in press
Prialnik, D., & Kovetz, A. 1984, ApJ, 281, 367
———. 1992, ApJ, 385, 665
Prialnik, D., & Shara, M. M. 1986, ApJ, 311, 172
———. 1995, AJ, in press
Prialnik, D., Shara, M. M., & Shaviv, G. 1978, A&A, 62, 339
———. 1979, A&A, 72, 192
Rogers, F. J., & Iglesias, C. A. 1993, private communication
Saizar, P., & Ferland, G. J. 1994, ApJ, 425, 755
Schwartzman, E., Kovetz, A., & Prialnik, D. 1994, MNRAS, 269, 323
Shara, M. M. 1981, ApJ, 243, 268
———. 1989, PASP, 101, 5
Shara, M. M., Livio, M., Moffat, A. F. R., & Orio, M. 1986, ApJ, 311, 163
Shara, M. M., Moffat, A. F. J., McGraw, T. J., Dearborn, D. S., Bond, H. E., Kemper, E., & Lamontagne, R. 1984, ApJ, 292, 763
Shara, M. M., Moffat, A. F. J., & Webbink, R. F. 1985, ApJ, 294, 271
Shara, M. M., Prialnik, D., & Kovetz, A. 1993, ApJ, 406, 220
Snijders, M. A. J., Batt, T. J., Roche, P. F., Seaton, M. J., Morton, D. C., Spoelstra, T. A. T., & Blades, J. C. 1987, MNRAS, 228, 329
Starrfield, S., Sparks, W. M., & Shaviv, G. 1988, ApJ, 325, L35
Starrfield, S., Sparks, W. M., & Truran, J. W. 1974a, ApJS, 28, 247
———. 1974b, ApJ, 192, 647
———. 1985, ApJ, 291, 136
Truran, J. W. 1990, in Physics of Classical Novae, ed. A. Cassatella & R. Viotti (Berlin: Springer), 373
Truran, J. W., Hayes, J., Shankar, A., & Livio, M. 1990, unpublished
Truran, J. W., Livio, M., Hayes, J., Starrfield, S., & Sparks, W. M. 1988, ApJ, 324, 345
Vogt, N. 1990, ApJ, 356, 609
Warner, B. 1987, MNRAS, 227, 23
Wheeler, J. C. 1992, in Evolutionary Processes in Interacting Binary Stars, ed. Y. Kondo, R. F. Sistero, & R. S. Polidan (Dordrecht: Kluwer), 225
Whelan, J., & Iben, I., Jr. 1973, ApJ, 186, 1007
Williams, R. E. 1994, ApJ, 426, 279
Williams, R. E., Sparks, W. M., Gallagher, J. S., Ney, E. P., Starrfield, S., & Truran, J. W. 1981, ApJ, 251, 221